Standard solar models and the uncertainties in predicted capture rates of solar neutrinos

John N. Bahcall

Institute for Advanced Study, Princeton, New Jersey 08540

Walter F. Huebner

Los Alamos National Laboratory, Los Alamos, New Mexico 87545

Stephen H. Lubow

Hewlett-Packard Corporation, Cupertino, California 95014

Peter D. Parker

Yale University, New Haven, Connecticut 06520

Roger K. Ulrich

University of California at Los Angeles, Los Angeles, California 90024

The uncertainties that affect the prediction of solar neutrino fluxes are evaluated with the aid of standard solar models. The uncertainties are determined from available data for all measured quantities that are known to affect significantly the neutrino fluxes; these include nuclear reaction rates, the solar constant, and the primordial surface composition of the sun. Uncertainties in theoretical quantities (such as the stellar opacity, the equation of state, and the rate of the proton-proton reaction) are estimated from the range of values in published state-of-the-art calculations. The uncertainty in each neutrino flux that is caused by a specified uncertainty in any of the parameters is evaluated with the aid of a series of standard solar models that were constructed for this purpose; the results are expressed in terms of the logarithmic partial derivative of each flux with respect to each parameter. The effects on the neutrino fluxes of changing individual parameters by large amounts can usually be estimated to satisfactory accuracy by making use of the tabulated partial derivatives. An overall "effective 3σ level of uncertainty" is defined using the requirement that the true value should lie within the estimated range unless someone has made a mistake. Effective 3σ levels of uncertainty, as well as best estimates, are determined for the following possible detectors of solar neutrinos: ^{2}H, ^{7}Li, ^{37}Cl, ^{71}Ga, ^{79}Br, ^{81}Br, ^{97}Mo, ^{98}Mo, ^{115}In, and electron-neutrino scattering. The most important sources of uncertainty in the predicted capture rates are identified and discussed for each detector separately. For the ^{37}Cl detector, the predicted capture rate is 7.6 ± 3.3 (effective 3σ errors) SNU. The measured production rate is (Cleveland, Davis, and Rowley, 1981) 2.1 ± 0.3 SNU (1σ error). For a ^{71}Ga detector, the expected capture rate is $106\,(1^{+0.12}_{-0.08})$ SNU (also effective 3σ errors). The relatively small uncertainty quoted for the ^{71}Ga detector is a direct result of the fact that ^{71}Ga is primarily sensitive to neutrinos from the basic proton-proton reaction, the rate of which is determined largely by the observed solar luminosity. The Caltech and Munster measured values for the cross-section factor for the reaction $^{3}\mathrm{He}(\alpha,\gamma)^{7}\mathrm{Be}$ are inconsistent with each other. The capture rates quoted above were obtained using the Caltech value for the cross-section factor. If the Munster value is used instead, then the predicted capture rate for the ^{37}Cl experiment is 4.95 ± 2.1 SNU (effective 3σ errors) and, for the ^{71}Ga experiment, 96.7 $(1^{+0.12}_{-0.08})$ SNU (effective 3σ errors). In order for the best-estimate value to agree with the observation of Davis (1978) of 2 SNU for the ^{37}Cl experiment, the cross-section factor $S_{34}(0)$ would have to be reduced by about 15σ to less than the Caltech value, i.e. to 7σ less than the Munster value. The characteristics of the standard solar model, constructed with the best available nuclear parameters, solar opacity, and equation of state, are presented in detail. The computational methods by which this and similar models were obtained are also described briefly. The primordial helium abundance inferred with the aid of standard solar models is $Y=0.25\pm0.01$. The complementary relation between observations of solar neutrinos and of the normal modes of oscillation of the sun is examined. It is shown that the splitting of the observed large-n, small-l, p-mode (five minute) oscillations of the sun primarily originates in the outer ten percent of the solar mass, while the neutrinos from ^{8}B beta decay originate primarily in the inner five percent of the solar mass. The solar luminosity, and the flux of neutrinos from the proton-proton reaction, come mostly from an intermediate region.

CONTENTS

I. INTRODUCTION

The discrepancy between observation and expectation for the ^{37}Cl solar neutrino experiment has stimulated many discussions of the significance of this disagreement. A central question that recurs in all of these discussions is: Could the disagreement be a result of errors in some of the input parameters? In this paper we provide a quantitative answer to this question, and also calculate for the proposed new solar neutrino experiments the range of capture rates that are consistent with standard solar models.

Models of the solar interior must be constructed with unusual detail and numerical accuracy in order to calculate reliably the implied neutrino fluxes. With the aid of our detailed solar models, we have calculated, and present in this paper, a variety of solar quantities that are interesting in their own right, such as the primordial helium abundance by mass fraction ($Y = 0.245 \pm 0.01$), the detailed run of the physical variables (see Table VII), and the relative contributions of the different regions of the sun to the observed frequency splitting of the p-mode (5-minute) oscillations (see Fig. 3).

We assume in this paper the conventional pictures of stellar evolution and neutrino propagation. We do not discuss the many interesting suggestions that have been made of how to modify the conventional ideas of stellar evolution in order to be in agreement with the results of the ^{37}Cl experiment. We also suppose that electron neutrinos produced in the solar interior are unaffected by either oscillations or decay on the way to the Earth from the sun. Thus our conventional calculations can be used as a standard for deciding whether or not solar neutrino experiments provide evidence for unexpected phenomena, either physical or astrophysical.

Different neutrino detectors will be sensitive in varying amounts to individual input parameters. It is important, therefore, to evaluate the sensitivity of the ^{37}Cl detector and also each of the other proposed solar neutrino detectors to possible changes in each of the important individual parameters (and neutrino fluxes) in order to sort out what each proposed detector can tell us either about properties of the solar interior or about the propagation characteristics of low energy neutrinos.

We have chosen to estimate the uncertainties at an overall "effective 3σ level of confidence" (corresponding to a greater than 0.997 level of confidence for purely statistical errors); in practice, this is equivalent to the requirement that if the true value lies outside the estimated range, someone has made a mistake. We use standard statistical techniques and the estimated numerical uncertainties, in order to determine the 3σ limits for measured quantities. Nevertheless, matters of judgment are important in this undertaking, especially in determining what is an effective 3σ range for a theoretically calculated quantity. In practice, we have most often taken theoretical uncertainties to be determined by the range in values in published state-of-the-art calculations. It is possible that we assign relatively larger errors for experimentally determined parameters (for which the uncertainties are more easily quantifiable) than we do for calculated parameters such as the opacity. However, the adopted procedure is as objective as any we can think of and has the advantage of simplicity. In the final analysis, our method for estimating errors is defined by the examples we discuss. In all cases, the procedures and assumptions we use to obtain the final uncertainties are stated explicitly. If the reader has a better (or just different) way of estimating the errors, then the reader can recalculate easily the uncertainties in all the predicted capture rates using the results and prescriptions described in this paper.

We have had to combine theoretical uncertainties with statistical (and possible systematic) errors in measured quantities. In doing so, we have adopted three rules. (1) Errors from different sources are combined incoherently (the total uncertainty is the square root of the sum of the squares of the individual uncertainties). (2) The effects of individual parameter uncertainties are determined by calculating stellar models with different values of the parameters of interest. (3) Only data published prior to July 1, 1981 are used (except for the recent papers on the $^{3}\mathrm{He}(\alpha,\gamma)^{7}\mathrm{Be}$ and $^{7}\mathrm{Li}(d,p)^{8}\mathrm{Li}$ cross-section factors that are discussed in Sec. II.A).

Many researchers use properties of the standard solar model for different applications; we have tabulated, therefore (in Table VII), the physical characteristics of our standard solar model in sufficient detail to be of use for a variety of purposes. We have also provided enough detail about the parameters and methods we have used in obtaining our standard model to enable workers with different stellar evolution programs to compare easily their results with ours.

The plan of this paper is given below. In Sec. II we evaluate the uncertainties that exist in nuclear parameters, in the solar constant, in the present-day surface composition of the sun, and in the stellar opacity. We also determine best estimates for each of these quantities and determine the less important uncertainties in the solar age and the interior equation of state. In Sec. III we tabulate the run of physical variables in our standard model (Table VII). We also present integral quantities, such as neutrino fluxes (Table VIII), the primordial helium abundance and its uncertainty [Eq. (17) and Table X], and the fraction of energy generated by the *p-p* and CNO cycles. The relative contributions of different regions of the sun to the splitting of the frequencies of the *p*-mode (large-n, small-l) five-minute oscillations are calculated and presented in Fig. 3. We also give in Table IX the computed solar luminosity and radius as a function of time. In Sec. IV we evaluate the partial derivatives of each of the neutrino fluxes with respect to the various parameters of interest; the results are presented in Tables XI–XIV. In Sec. V these partial derivatives are used to determine the uncertainties in the predicted solar neutrino fluxes and in the expected capture rates for detectors composed of ^{2}H, ^{7}Li, ^{37}Cl, ^{71}Ga, ^{79}Br, ^{81}Br, ^{97}Mo, ^{98}Mo, ^{115}In, and for electron-neutrino scattering. The results are summarized in Tables XV and XVI. Also presented in this section are the best current estimates for the predicted capture rates with each of these targets; these results are summarized in Table XVIII. In Sec. VI we summarize our main results and conclusions.

All of the neutrino capture rates in this paper are expressed in solar neutrino units of 1 SNU $\equiv 10^{-36}$ captures per target atom per second, a unit introduced partially in jest by Bahcall (1969b).

This paper is part of a series of studies of solar neutrino models that began in 1964 (references to other papers in this series are given in the caption of Fig. 4).

For the reader's convenience, we list in the Prefatory Table some numerical values for solar quantities. We do not define or defend these values in this section since that is done in the remainder of the paper.

The proton-proton chain of nuclear reactions provides, according to the standard solar model, more than ninety-eight percent of the energy required to produce the presently observed solar luminosity. Also, most of the observable solar neutrinos are produced by reactions in this chain. We show in Table I the important reactions involved in this chain, the relative frequency of their occurrence, and the most significant associated neutrino sources. The neutrino spectrum predicted by the standard solar model is shown in Fig. 2.

This paper contains detailed results of interest to specialists in different fields. A partial list of the specialities that are involved in our discussions includes: experimental nuclear physics, atomic physics (opacity calculations), solar oscillations, stellar evolution, cosmology (the primordial helium abundance), particle physics (neutrino oscillations), and, of course, solar neutrino experiments. The reader may use his time most profitably by first scanning the table of contents for topics of interest to him, reading only the sections of special interest, and then skipping to Sec. VI to read our summary of the main results and conclusions. In fact, the reader with little time to spend might prefer to jump immediately to the conclusions to see if the results justify further effort.

Prefatory table of some important solar parameters.

Parameter	Value
Luminosity	3.86×10^{33} erg sec^{-1}
Mass ($M_\odot$)	1.99×10^{33} g
Radius ($R_\odot$)	6.96×10^{10} cm
Moment of Inertia	7.00×10^{53} g cm^2
Depth of convective zone	$0.27\,R_\odot(0.02M_\odot)$
Age	$\geq 4.55 \times 10^{9}$ yr
Central density	156 g cm^{-3}
Central temperature	15.5×10^{6} K
Central hydrogen abundance by mass	0.355
Effective (surface) temperature	5.78×10^{3} K
Primordial helium abundance by mass	0.25 ± 0.01
Primordial ratio of heavy elements to hydrogen mass	0.0228
Neutrino flux from *p-p* reaction	6.1×10^{10} cm^{-2} sec^{-1}
Neutrino flux from ^{8}B decay	5.6×10^{6} cm^{-2} sec^{-1}
Fraction of energy from *p-p* chain	0.985
Fraction of energy from CNO cycle	0.015

II. INPUT PARAMETERS

In this section we estimate a preferred value and an equivalent 3σ uncertainty for each of the parameters that affects in an important way the solar neutrino fluxes calculated from standard solar models. There have been many previous discussions of the parameters and their uncertainties, including studies by Bahcall (1964); Sears (1964); Parker, Bahcall, and Fowler (1964); Fowler, Caughlan, and Zimmerman (1967); Salpeter (1968); Iben (1968); Bahcall and Shaviv (1968); Bahcall, Bahcall, and Ulrich (1969); Bahcall and Ulrich (1970); Bahcall and Sears (1972); Fowler (1972); Ulrich (1974); Fowler; Caughlan, and Zimmerman (1975); Parker (1978); Rolfs and Trautvetter (1978); Bahcall (1979); Bahcall *et al.* (1980); Trautvetter (1981); and Parker (1982). The present discussion is intended to be both explicit and contemporary, bringing previous discussions up to date and to a certain extent clarifying them and making them more complete and accurate. We make our own detailed evaluations of the uncertainties in the important experimental quantities, since in some cases the original analyses have not been explicit or correct.

TABLE I. The proton-proton chain. The numbers in parentheses are the percentages of terminations of the chain in which various reactions are calculated to occur for the standard solar model discussed in Sec. III.

	Reaction	% of terminations	Maximum neutrino energy (MeV)
	$p+p\rightarrow{}^2\mathrm{H}+e^+ +\nu$	(99.75)	0.420
	or		
	$p+e^-+p\rightarrow{}^2\mathrm{H}+\nu$	(0.25)	1.44(monoenergetic)
	${}^2\mathrm{H}+p\rightarrow{}^3\mathrm{He}+\gamma$	(100)	
I.	${}^3\mathrm{He}+{}^3\mathrm{He}\rightarrow{}^4\mathrm{He}+2p$	(86)	
	or		
II.	${}^3\mathrm{He}+{}^4\mathrm{He}\rightarrow{}^7\mathrm{Be}+\gamma$		
	${}^7\mathrm{Be}+e^-\rightarrow{}^7\mathrm{Li}+\nu$	(14)	0.861 (90%), 0.383 (10%) (both monoenergetic)
	${}^7\mathrm{Li}+p\rightarrow 2{}^4\mathrm{He}$		
	or		
III.	${}^7\mathrm{Be}+p\rightarrow{}^8\mathrm{B}+\gamma$		
	${}^8\mathrm{B}\rightarrow{}^8\mathrm{Be}^*+e^+ +\nu$	(0.015)	14.06
	${}^8\mathrm{Be}^*\rightarrow 2{}^4\mathrm{He}$		

A. Nuclear reactions

The basic quantity of interest for all of the nuclear reactions we discuss is the low-energy cross-section factor $S(E)$ defined by (see, for example, Clayton, 1968)

$$S(E) = \sigma(E)E\exp(2\pi Z_1 Z_2 e^2/\hbar v), \quad (1)$$

where $\sigma(E)$ is the cross section at the center-of-mass energy E, Z_1Z_2 is the product of the atomic numbers of the interacting particles, and v is their relative velocity. We discuss separately each of the most important reactions in the proton-proton chain, which is the dominant source of energy and neutrino production in the sun. The CNO reactions are discussed only briefly, following Parker (1982).

1. $p + p \rightarrow {}^2\mathrm{H} + e^+ + \nu_e$

The effective cross-section factor for the proton-proton reaction can be written (Bahcall and May, 1969):

$$S_{\mathrm{eff}} = S(E=0)[1 + 0.417\tau^{-1} + 12.6\tau^{-2} + 36.6\tau^{-3}], \quad (2)$$

where $\tau = 33.80\,T_6^{-1/3}$ and T_6 is the temperature in units of 10^6 K. The last two terms of the factor enclosed in brackets represent a correction term proportional to the logarithmic derivative of the cross-section factor evaluated at zero energy, $(S^{-1}dS/dE)_{E=0}$. The best estimate of $(S^{-1}dS/dE)_{E=0}$ is still that of Bahcall and May, so that the bracketed terms in Eq. (2) are unaltered.

The contributions to S_{eff} that arise from meson exchange are denoted usually by $(1+\delta)^2$. We write, for convenience,

$$S(E=0) = S(E=0;\delta=0)\,(1+\delta)^2.$$

The Bahcall-May values, and uncertainties, for $S(E=0;\delta=0)$ and $(S^{-1}dS/dE)$ have been used for most recent solar neutrino calculations. In particular, $S_{B-M}(E=0;\delta=0) = (3.78\pm0.15)\times10^{-25}$ MeV b was the standard value used in papers in this series from 1968 (Bahcall, Bahcall, and Shaviv, 1968) until 1980 (Bahcall *et al.*, 1980). However, recent experimental results justify a reexamination of this value (see Bahcall *et al.*, 1980).

The value of $S(E=0;\delta=0)$ is proportional to the square of the effective Gamow-Teller coupling constant, which has usually been determined from the ratio of the neutron ft value to the ft value for 0^+ to 0^+ superallowed transitions between $T=1$ states. The values for the 0^+ to 0^+ superallowed transitions have been determined by many accurate experiments and are well known. Including radiative corrections as indicated by Blin-Stoyle and Freeman (1970), one has (see, for example, Vonach *et al.*, 1977): $(ft_{1/2})_{0^+\,0^+} = (3087 \pm 3.5)$ sec.

The recent measurements of the neutron half-life are not in good agreement with each other. Sosnovski *et al.* (1959) quote (11.70 ± 0.3) min; Christensen *et al.* (1972) obtain $t_{1/2} = (10.62\pm0.16)$ min; Bondarenko *et al.* (1979) find $t_{1/2} = (10.13\pm0.09)$ min. Most recently, Byrne *et al.* (1980) determined $t_{1/2} = (10.82 \pm 0.21)$ min. Bahcall and May used the earlier value of $t_{1/2} = 10.80$ min given by Christensen *et al.* (1967). Systematic errors have been treated differently by each

group and may be more important than the recognized statistical errors.

We adopt the average of the above four independent measurements, i.e., $t_{1/2} = 10.82^{+0.9}_{-0.7}$ min. The indicated uncertainty spans the entire range of modern measurements of the neutron half-life. Because each of the groups used a different method for estimating the uncertainties, and because systematic errors are probably important in the difficult experiments being discussed here, formal probabilities cannot be attached to the range of values we quote for the neutron lifetime. However, we expect that the extreme values of the range correspond approximately to 3σ excursions.

The value of the neutron lifetime adopted in the previous paragraph corresponds (Bahcall, 1966a; Bahalla, 1966) to $ft_{1/2}(n) = 1115$ sec, when a 1.5% radiative correction (see Blin-Stoyle and Freeman, 1970) is included. The formal range of (G_A/G_V) that is implied by the above-described range of neutron lifetimes and 0^+ to 0^+ decay rates is $G_A/G_V = 1.23 \pm 0.05$.

In addition to making use of the neutron lifetime, there are two other ways of determining the square of the effective Gamow-Teller coupling constant. They involve (1) a measurement of the electron-nuclear spin correlation in the decay of polarized neutrons (see, for example, Krohn and Ringo, 1975) and (2) the electron-neutrino correlation determined from the energy spectrum of the recoil proton (see, for example, Dobrozemsky *et al.*, 1975). These measurements yield values of (G_A/G_V) that are consistent with the range determined above from the half-life of the neutron.

We may write, therefore,

$$S(E=0;\delta=0) = 1.204 \left[\frac{10.82 \text{ min}}{t_{1/2}(n)}\right] S_{B-M}(E=0;\delta=0) \times \left[1 - 0.1806 \left[\frac{t_{1/2}(n)}{10.82 \text{ min}}\right]\right] \quad (3)$$

or, equivalently,

$$S(E=0;\delta=0) = 0.987 S_{B-M}(E=0)(G_A/1.23\,G_V)^2.$$

For $t_{1/2}(n) = 10.82$ min, one has

$$S(E=0;\delta=0) = 0.99 S_{B-M}(E=0;\delta=0).$$

The electromagnetic radiative corrections are particularly easy to evaluate in the form appropriate to Eq. (3). One needs only the ratio of the correction for the proton-proton reaction to the correction for the neutron decay. This ratio may be taken to be unity within the accuracy of interest here (cf. Blin-Stoyle and Freeman, 1970).

The most recent calculation of the π- and ρ-meson exchange corrections to the *p-p* reaction rate yields (Bargholtz, 1979) a somewhat smaller value, $\delta = 0.01^{+0.01}_{-0.006}$ than previous calculations which gave values of δ of order 0.03 to 0.04 from pion exchanges only (see, for example, Blin-Stoyle and Papageorgiou, 1965; Gari and Huffman, 1972; Dautry, Rho, and Riska, 1976). The detailed calculations of Bargholtz include, for the first time, both π and ρ exchanges, as well as monopole form factors (see also Gari, 1978).

For the error estimates in this paper, we adopt the conservatively large range of $\delta = 0.02^{+0.02}_{-0.015}$, which is consistent with practically all of the published theoretical estimates of exchange corrections.

The situation may be summarized in the following suggestive form:

$$S(E=0) = S_{B-M}(E=0;\delta=0)(1 \pm 0.025) \times (0.987^{+0.08}_{-0.09})(1.02^{+0.02}_{-0.015})^2.$$

The uncertainty in the first parenthesis arises from the estimated uncertainty (by Bahcall-May, 1969) in the nuclear matrix element; the second (and largest) uncertainty represents the extreme range of experimental values for the neutron lifetime; the third uncertainty arises from the imperfectly known corrections for mesonic exchanges. In all cases, we have allowed the maximum plausible range for the parameter in question that is consistent with published estimates. The individual uncertainties have been combined as independent errors.

Our final result may be written as

$$S_{p-p}(E=0) = 3.88(1 \pm 0.09) \times 10^{-25} \text{MeV b}. \quad (4)$$

The indicated uncertainty in the *p-p* reaction rate corresponds (see Sec. V.B) to a significant uncertainty in the prediction of the neutrino capture rate for the ^{37}Cl experiment. However, this lack of precision is not very important for experiments that are primarily sensitive to *p-p* neutrinos.

2. $p + e^- + p \rightarrow {}^2\text{H} + \nu_e$

The rate for the *pep* reaction is proportional to the rate of the basic *p-p* reaction that was discussed in the previous subsection. Bahcall and May (1969) derived the following approximate formula for the ratio of the rates of the *pep* and *p-p* reactions:

$$R_{p+e+p} \approx 5.51 \times 10^{-5}\, \rho(1+X) T_6^{-1/2}\, (1 + 0.02 T_6) R_{p-p}. \quad (5)$$

Here ρ is the density in g cm^{-3}, X is the fraction of hydrogen by mass, and T_6 is the temperature in millions of degrees Kelvin. This formula for the ratio is accurate to about one percent for all solar temperatures in the range $10 < T_6 < 16$; this is the relevant temperature range for the production of solar neutrinos. The main uncertainty in the rate of the relatively rare *pep* reaction is caused by the previously discussed uncertainty in the value of the effective cross-section factor for the *p-p* reaction.

3. ${}^2\text{H} + p \rightarrow {}^3\text{He} + \gamma$

The cross section for this reaction has been measured by Griffiths, Lal, and Scarfe (1963) down to a center-of-

mass energy of 15 keV. The extrapolation to lower energies determines the cross-section factors

$$S_{12}(0) = (2.5 \pm 0.4) \times 10^{-4}\,\text{keV b}, \tag{6a}$$

$$(dS_{12}/dE)_{E=0} = +7.9 \times 10^{-6}\,\text{b}. \tag{6b}$$

The (p,γ) reaction is the only important deuterium-burning reaction (Parker, Bahcall, and Fowler, 1964). The quoted 1σ uncertainty in Eq. (6a) is not important for calculations of solar neutrino fluxes because this is the only important deuterium-burning reaction in the proton-proton chain and because the *p-p* reaction, which occurs via a weak interaction, is much slower.

4. $^3\text{He} + {}^3\text{He} \rightarrow {}^4\text{He} + 2p$

This reaction is the dominant way of terminating the proton-proton chain in the sun. The low-energy cross sections have been measured accurately in a series of important experiments that cover the range from about 1.3 MeV to as low as 33 keV (see especially Tombrello, 1967; Dwarakanath and Winkler, 1971; and Dwarakanath, 1974).

Previous estimates of the uncertainty in the value of the low-energy cross-section factor S_{33} all appear to have been determined by least-squares fits to the data. The meaning of the quoted error is not stated explicitly in the experimental papers, but the final uncertainties quoted usually appear to be derived from an approximately 1σ deviation of the overall theoretical curve for S_{33} from the measured values as a function of energy, assuming a theoretical form for S_{33} that is a quadratic function of energy. However, this procedure is not the best way to determine the value of S_{33} at essentially zero energy, which is the quantity of interest here, since linear and quadratic terms do not contribute significantly at the very low thermal energies that occur in the solar interior.

The correct procedure (see, for example, Avni, 1978; Cash, 1976) is to find the minimum χ^2 for each value of $S_{33}(0)$, allowing the linear and quadratic fitting parameters to be whatever gives the best fit to the data. Let the minimum χ^2 at energy E be denoted by $C(E)$ and the absolute minimum of this set of minimum χ^2's be denoted by C_{Min}. Then the region corresponding to a given confidence level "*con*" is the set of points for which the difference $C(E) - C_{Min}$ is less than or equal to $\chi^2(con)$, where χ^2 is the usual χ^2 distribution. Thus, for example, the 3σ uncertainty is obtained by finding the extreme values of S_{33}, $[S_{33}^{MAX}(0)$ and $S_{33}^{MIN}(0)]$, for which the computed χ^2 values just exceed by nine the χ^2 for the best-fitting value of the cross-section factor (i.e., the value of S_{33} that yields C_{Min}).

TABLE II. Some best-fitting parameters and values of χ^2 for the ^3He-^3He reaction. The values of S_1 and S_2 are the best-fitting parameters for the specified $S(0)$ and χ^2 is the corresponding value of χ^2.

$S(0)$	$S_1(0)$	$S_2(0)$	χ^2
3.5	+3.25	−2.5	45.1
4.0	+1.5	−1.5	25.8
4.3	+0.5	−0.75	19.3
4.5	−0.25	−0.25	16.7
4.6	−0.6	−0.1	16.0
4.7	−0.9	+0.1	15.6
4.9	−1.5	+0.5	16.1
5.0	−2.0	+7.5	17.7
5.5	−3.5	+1.75	26.8
6.0	−5.25	+3.0	46.0

We have computed the best-fitting values of the quadratic function $S(E) = S(0) + S_1(0)E + S_2(0)E^2$ in the manner described above. We used in the first instance the published data points available from Bacher and Tombrello (as quoted in Tombrello, 1967, and in Dwarakanath and Winkler, 1971), Dwarakanath and Winkler (1971), and Dwarakanath (1974) over the full range from 1.35 MeV to about 0.04 MeV for which there exist accurate data. In weighting these data points, we have assumed, following the estimates in the original papers, that the uncertainties were $\pm 10\%$ in the measured values of $S(E)$ for all the data points above 100 keV and $\pm 20\%$ for data points below 100 keV. The data points below 40 keV were not included because the uncertainties in the inferred values of S were very large.

The results are shown in Table II. By inspecting this table, the reader can verify that the computed values of χ^2 initially increase rather slowly as one departs from the cross-section factor for which the minimum χ^2 is achieved until they suddenly start to increase rapidly. Thus the estimates of the uncertainties are rather well determined and do not depend very sensitively on details of the analysis.

The best-fitting value of the cross section factor with the appropriate 3σ confidence levels is

$$S_{33}(0) = 4.7^{+0.8}_{-0.7}\,\text{MeV b}. \tag{7}$$

We have also done numerical experiments to see how sensitive the above-quoted estimates are to changes in various data. The results obtained, for example, by ignoring all data below 100 keV are $S_{33}(0) = 5.5^{+0.75}_{-1.25}$ keV b, consistent with the analysis of Dwarakanath and Winkler (1971).

The uncertainties derived above are not large enough to affect significantly the predictions of solar neutrino fluxes.

No evidence has been found for the *a priori* unlikely possibility (Fowler, 1972; Fetisov and Kopysov, 1972) of a low-energy resonance in this reaction (see, for example, Parker *et al.*, 1973; Halbert, Hensley, and Bingham, 1973; and Dwarakanath, 1974).

5. $^3\text{He} + {}^4\text{He} \rightarrow {}^7\text{Be} + \gamma$

For more than a decade, the standard value of $S_{34}(0)$ was determined by combining two independent data sets into one and fitting them with a second-order polynomial in energy. The cross section was measured by Parker

and Kavanagh (1963) in the energy range $181 \leq E_{cm} \leq 2493$ keV and by Nagatani, Dwarakanath, and Ashery (1969) in the range $164 \leq E_{cm} \leq 245$ keV. These later authors estimated a value of $S_{34}(0) = 0.61 \pm 0.07$ keV b (1σ error) from a fit to the combined data.

The procedure that led to the value of 0.61 keV b is not the best way to analyze the available data. The two measurements were performed with different apparatus and therefore involve independent sources of systematic errors. Moreover, the two data sets have little overlap in energy, so that dS/dE was determined primarily by a comparison between the low-energy (Nagatani *et al.*, 1969) data and the higher-energy (Parker and Kavanagh, 1963) data. Viewed separately, neither of these two experiments is adequate to measure dS/dE at low energies; the Parker-Kavanagh data are not sufficiently accurate at low energy, while the Nagatani *et al.* data do not cover a large enough energy range.

At the present time, the procedure that seems most reasonable to us is to use each of these data sets to determine separate values of $S_{34}(0)$, adopting a value of dS/dE that is based on some independent measurement, calculation, or assumption.

We have made use of the direct-capture cluster-model calculation (Tombrello *et al.*, 1963) to determine the energy dependence of $S(E)$. The Parker-Kavanagh and Nagatani *et al.* data sets then determine, respectively, $S(0) = 0.47 \pm .05$ keV b and 0.57 ± 0.06 keV b (1σ uncertainty).

We adopt the average of the two determinations given above,

$$S_{34}(0) = 0.52 \pm 0.15 \text{ keV b}, \tag{8}$$

where the uncertainty is now a 3σ value. The accuracy of the direct-capture cluster-model calculation is supported by the remarkably good agreement (Tombrello *et al.*, 1963) between the calculation and the Parker-Kavanagh data over the range 500 keV $< E_{cm} <$ 2500 keV, in which those data are sufficiently accurate to test the model.

The value of S_{34} given in Eq. (8) was first used by us in the calculations described in Bahcall *et al.* (1980).

Stimulated by the preliminary report by Rolfs (1979) of measurements which seemed to indicate a nearly flat energy dependence of $S(E)$ for the ^{3}He $(\alpha,\gamma)^7$Be reaction over the range 150 keV $\leq E_{cm} \leq$ 1700 keV [in contrast to the earlier experimental (Parker *et al.*, 1963) and theoretical (Tombrello *et al.*, 1963) results noted above], there has recently been a flurry of renewed interest in this reaction. The original direct-capture-model calculation (Tombrello *et al.*, 1963) has been reexamined and substantially refined by several groups (Barker, 1979; Kim *et al.*, 1981; Liu *et al.*, 1981; Williams *et al.*, 1981; Kalnin *et al.*, 1980); the results of all of these new calculations are in good agreement with the results of the 1963 calculation, predicting values of $S^{-1}\, dS/dE$ between -0.50 MeV^{-1} and -0.60 MeV^{-1} at low energies. In the two years since Rolfs's preliminary report, extensive additional experiments have been carried out at Munster (Rolfs, 1981) and at Caltech (Osborne *et al.*, 1981) to measure the low-energy behavior of $S(E)$ for this reaction. The results of both of these new measurements are now in good agreement with the energy dependence predicted by the direct-capture calculations. Several experimental groups, including the Caltech and Munster collaborations, are currently investigating the *absolute* normalization of the cross section measurements.

A recent (12/1981) preprint from the Munster group by Krawinkel *et al.* (1982) reports a result of $S_{34}(0) = 0.30 \pm 0.03$ keV b on the basis of measurements with a differentially pumped gas target and a gas jet target. At the same time, however, preliminary results from the Caltech group (Osborne, *et al.*, 1981) give $S_{34}(0) = 0.51 \pm 0.03$ keV b on the basis of their measurements with a differentially pumped gas target and $S_{34}(0) = 0.56 \pm 0.03$ keV b on the basis of a measurement of the ^{7}Be activity. A similar activity measurement is currently being performed at Munster. The uncertainties quoted from these recent preprints are all 1σ errors.

The results of the Caltech and Munster groups are not consistent with each other. Nevertheless, we must adopt a particular value in order to calculate the expected neutrino capture rates. In what follows, we assume for our standard estimates the value given by Eq. (8) above (which is consistent with the new Caltech values), but indicate where relevant the capture rates that are implied by the Munster value for $S_{34}(0)$. Filipone and Schramm (1982) have adopted $S_{34}(0) = 0.52^{+0.15}_{-0.23}$ keV b, where the indicated errors were used by them as 1σ errors. The errors assumed by Filipone and Schramm are much larger than are quoted by any of the experimental groups and imply, if interpreted naively at the 3σ level of confidence, the possibility of a *negative* cross-section factor.

6. $e^- + {}^7\text{Be} \rightarrow {}^7\text{Li} + \nu_e$

The rate at which ^{7}Be captures an electron in a stellar interior can be written approximately in the following convenient form (Bahcall and Moeller, 1969):

$$\lambda = 4.62 \langle B \rangle 10^{-9} (\rho/\mu_e) T_6^{-1/2} \times [1 + 0.004(T_6 - 16)] \text{ sec}^{-1}, \tag{9}$$

where μ_e is the mean electron molecular weight $[\approx 2/(1 + X)]$, ρ is the total density in g cm^{-3}, and T_6 is the temperature in units of 10^6 K. The quantity $\langle B \rangle$ represents the enhancement of the continuum capture rate (Bahcall, 1962) by bound electron capture (Iben, Kalata, and Schwartz, 1967).

The numerical approximation represented by the last bracketed expression in Eq. (9) is accurate to 1% for $10 \leq T_6 \leq 16$.

The enhancement factor $\langle B \rangle$ was first calculated by Iben *et al.* (1967). The standard result that has been used for more than a decade by nearly all authors is the following value given by Bahcall and Moeller (1969):

$$\langle B \rangle_{1969} = 1.205 \pm 0.01, \quad (10)$$

which was based on detailed calculations using three, then-current, standard stellar models. It was noted at the time that for a completely mixed model $\langle B \rangle = 1.25$.

We have recalculated $\langle B \rangle$ for two stellar models discussed by Bahcall *et al.* (1980), the so-called standard model and the model with $S_{34} = 0.34$ keV b. We find

$$\langle B \rangle_{1981} = 1.192 \pm 0.003. \quad (11)$$

We also find $\langle B^{-1} \rangle^{-1} = \langle B \rangle$ to the limit of our numerical accuracy.

We therefore use Eq. (9) with $\langle B \rangle = 1.20$ for the total rate of electron capture by ^{7}Be. We estimate for standard models an uncertainty of the order of 2% in this rate because of numerical approximations made in deriving $\langle B \rangle$ and the last bracketed term in Eq. (9). Much larger uncertainties have sometimes been estimated in the past (cf., Ulrich, 1974), but without explicit justification.

7. $p + {}^7\text{Be} \rightarrow {}^8\text{B} + \gamma$

More than two-thirds of the counting rate predicted with a standard solar model for the ^{37}Cl solar neutrino experiment is from neutrinos produced by ^{8}B beta decay (see Bahcall, 1964a, and the discussion in Sec. III–V and Table XVII). The ^{8}B nuclei are produced by the reaction $^7\text{Be}(p,\gamma)^8\text{B}$, a reaction that is so rare that it does not affect the structure of the star.

The flux of neutrinos from ^{8}B beta decay is also expected, on the basis of the standard solar model, to be the dominant contributor to the capture rate in the ^{2}H, ^{7}Li, and electron-neutrino scattering experiments (see Sec. V). We review below the main uncertainties in the determination of the rate of this important reaction $^7\text{Be}(p,\gamma)^8\text{B}$ in the solar interior.

Five independent experimental studies of this reaction have been reported (Kavanagh, 1960; Parker, 1966, 1968; Kavanagh *et al.*, 1969, and Kavanagh, 1972; Vaughn *et al.*, 1970; Wiezorek *et al.*, 1977). Low-energy cross sections are determined primarily by two of these studies, the Caltech measurements (Kavanagh *et al.*, 1969; Kavanagh, 1972) and the Brookhaven measurements (Parker, 1966; Parker, 1968). [The 1960 measurements of Kavanagh (1960) included data at only two energies ($E_p = 800$ and 1400 keV), with an accuracy of only $\pm 40\%$. The measurement of Wiezorek *et al.* (1977) at Munster was done at only one energy, with an uncertainty of $\pm 25\%$. The measurements of Vaughn *et al.* (1970) at Lockheed were limited to bombarding energies above 950 keV.] The Lockheed cross sections are consistently about 30% smaller than the Brookhaven and Caltech cross sections in the overlapping energy range 1 MeV $< E_p <$ 3 MeV. The target matrix in the Lockheed experiment was much thicker, and alpha-particle energy resolution was much poorer, than for the Brookhaven or Caltech experiments, making the Lockheed data more difficult to analyze cleanly and reliably. There is good agreement between the Brookhaven and Caltech data. We have adopted, therefore, the Brookhaven and Caltech results. An average of these three normalizations (Brookhaven, Caltech, and Lockheed) would reduce our recommended value (see below) by about 10%.

The ^{7}Be target thicknesses in both the Brookhaven and Caltech experiments [as well as in the experiments reported by Kavanagh (1960) and Vaughn *et al.* (1970)] were determined by measuring the rate of ^{7}Li production in the target from the decay of ^{7}Be. The amount of ^{7}Li is measured using the $^7\text{Li}(d,p)^8\text{Li}$ reaction, for which the absolute cross section at its 770-keV resonance has been measured independently by several groups. However, the results for this (d,p) cross section show considerable scatter [211 ± 15 mb (Parker, 1966); 181 ± 8 mb (Schilling *et al.*, 1976); 174 ± 16 mb (Mingay, 1979); 163 ± 15 mb (Kavanagh, 1960—based on the $^7\text{Li}(p,p)$ elastic cross-section measurements of Warters *et al.*, 1953; Lerner *et al.*, 1969; Brown *et al.*, 1973); and 138 ± 20 mb (McClenahan *et al.*, 1975)], and it is clearly essential that a *careful* remeasurement be made of this number (see Barker, 1980). A weighted average of the above results yields 176 mb.

After this analysis was completed, two recent preprints were received (12/1981), reporting measurements of the $^7\text{Li}(d,p)^8\text{Li}$ cross section. Elwyn *et al.* (1982) have measured the angular distributions of the protons from this reaction and have determined $\sigma_{\text{TOTAL}} = 146 \pm 13$ mb; Filippone *et al.* (1982) have measured the delayed alpha particles from the decay of ^{8}Li and have inferred a value of $\sigma_{\text{TOTAL}} = 148 \pm 12$ mb. The inclusion of these two results in the weighted average yields a total cross section of 169 mb, in reasonable agreement with the previously determined weighted average of 176 mb.

However, the spread in the reported values for the total cross section in the seven references quoted above is larger than would be expected on the basis of the errors estimated by the individual groups. We have therefore chosen to use in the analysis quoted below the *arithmetical* mean of all the quoted total cross-section measurements and have taken the effective 3σ error to be one-half the total spread in quoted cross-section measurements. We thus adopt for the $^7\text{Li}(d,p)^8\text{Li}$ cross section the value $\sigma_{\text{TOTAL}} = 166 \pm 37$ mb (3σ error). Further experimental work on the total cross section of this reaction would be important.

We have reanalyzed all of the Brookhaven and Caltech $^7\text{Be}(p,\gamma)^8\text{B}$ data in order to determine the uncertainties associated with their measurements of the bombarding energy, the yield, and the target thickness [including the uncertainty in the $^7\text{Li}(d,p)$ cross section]. We are grateful to R. W. Kavanagh for providing us with the original data from his 1969 experiment.

The inferred low-energy cross-section factor depends upon the form of the extrapolation that is adopted. We follow the usual procedure of extrapolating the measured results using the behavior predicted by a direct-radiative-capture model for the reaction (Tombrello,

TABLE III. Cross-section factors for the CNO cycle. The uncertainties indicated in parentheses are estimated 1σ errors and have been calculated using the data given in the original experimental papers.

Reaction	S(0) (MeV b)	S' (0) (b)	$S''(0)$ (b/MeV)	Reference
$^{12}C(p,\gamma)^{13}N$	$1.45(1\pm0.15)\times10^{-3}$	2.45×10^{-3}	6.80×10^{-2}	Rolfs and Azuma (1974)
$^{13}C(p,\gamma)^{14}N$	$5.50(1\pm0.15)\times10^{-3}$	1.34×10^{-2}	9.87×10^{-2}	Fowler *et al.* (1967)
$^{14}N(p,\gamma)^{15}O$	$3.32(1\pm0.12)\times10^{-3}$	-5.91×10^{-3}	9.06×10^{-3}	Fowler *et al.* (1975)
$^{15}N(p,\gamma)^{16}O$	$6.4\ (1\pm0.09)\times10^{-2}$	3×10^{-2}	4.0	Rolfs and Rodney (1974)
$^{15}N(p,\alpha)^{12}C$	78.0 (1 ± 0.17)	351	1.11×10^{4}	Zyskind and Parker (1979)
$^{16}O(p,\gamma)^{17}F$	$9.4\ (1\pm0.16)\times10^{-3}$	-2.3×10^{-2}	6.0×10^{-2}	Rolfs (1973)

1965; Christy and Duck, 1961; Williams and Koonin, 1981) which predicts a rise in the cross-section factor $S(E)$ as E_{cm} is reduced from 100 keV towards zero energy. A particularly simple derivation of this predicted behavior has been given recently by Williams and Koonin (1981). The results of our reanalysis are

$$S_{17}(0) = 0.029 \pm 0.010 \text{ keV b}, \tag{12a}$$

$$S'_{17}(0) \approx -3\times10^{-5} \text{ b}, \tag{12b}$$

where $S'_{17}(0)$ is the first derivative of the cross-section factor at zero energy. The zero-energy intercept and slope given in Eq. (12) describe the model curve only at very low energies, i.e., $E_{cm} \lesssim 100$ keV. The indicated 3σ net uncertainty in $S_{17}(0)$ arises almost equally from the individual uncertainties associated with the $^7Li(d,p)^8Li$ cross section, the determination of the relative ^7Li production as a function of time in the various targets, and the measurement of the beam energy and the yield. Barker (1980) has considered some theoretical models, based on the $^7Li(n,\gamma)^8Li$ capture reaction, in which $S_{17}(0) = 0.018 \pm 0.04$ keV b.

It is instructive to calculate the 3σ uncertainty in the value of $S_{17}(0)$ using only a linear function of energy, without the upturn in $S(E)$ predicted by the direct-capture model. Fitting all the data below 450 keV in the center of mass frame, we find $S_{17}(0) = 0.0245 \pm 0.009$ keV b.

The data, together with the fits of the direct-capture model and the simple linear function, are all shown in

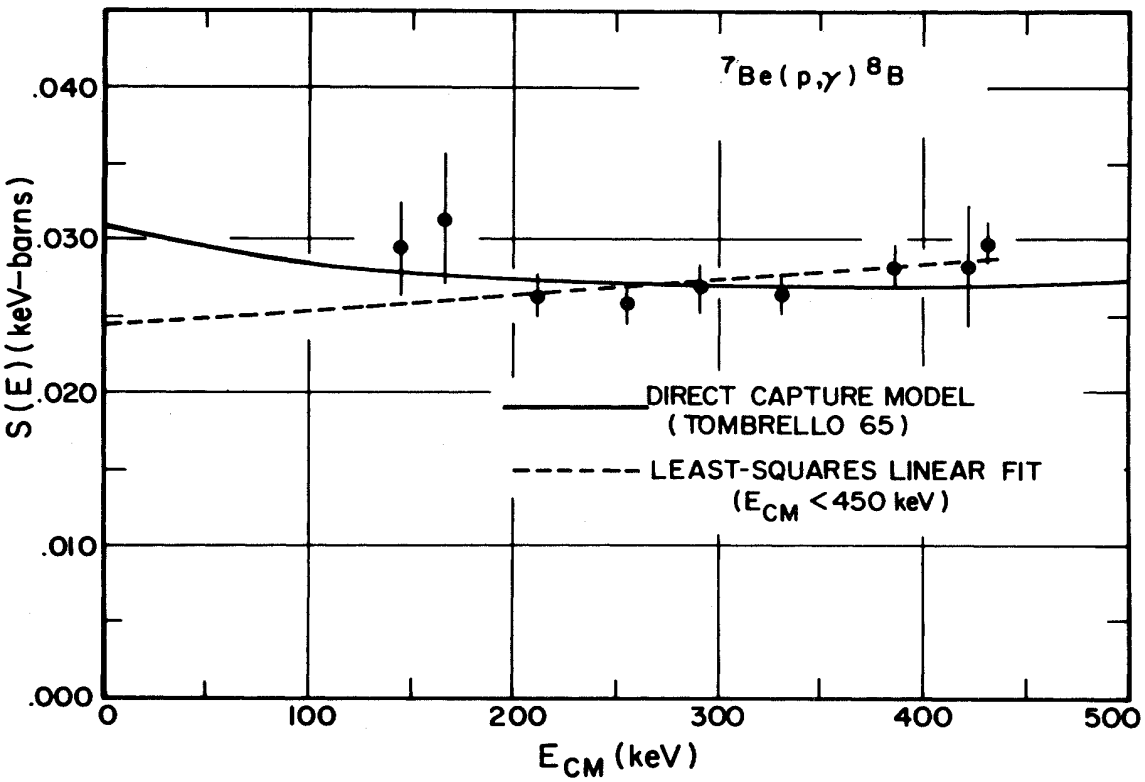

FIG. 1. Comparison of the direct-capture model (Tombrello, 1965; Williams and Koonin, 1981) and the least-squares-linear fit to the low-energy ($E_{cm} \leq 450$ keV) measurements of the $^7Be(p,\gamma)^8B$ cross section.

Fig. 1. The direct-capture model used in this analysis has been validated in the S_{34} studies described in subsection II.A.5 above; the comparison of the two curves in Fig. 1 makes clear the importance of having a reliable physical theory for use in extrapolating measured cross sections to very low energies.

8. The CNO cycle

Nuclear energy generation via the carbon-nitrogen cycle (see Bethe, 1939) accounts for only a small percentage ($\approx 1.5\%$) of the total fusion energy liberated in standard solar models. Moreover, the results of the ^{37}Cl experiment can be used to establish an observational upper limit of order 10% or less of the present solar luminosity that could be supplied by the CNO cycle (see Bahcall *et al.*, 1968; Davis *et al.*, 1968; Bahcall, 1979). Therefore, for most of the proposed solar neutrino experiments, the fluxes predicted for ^{13}N and ^{15}O neutrinos are not expected to be very important, although a ^{7}Li experiment would be sensitive to CNO neutrinos (Bahcall, 1978).

The low-energy cross sections for reactions in this cycle are known sufficiently accurately to enable us to calculate standard solar models without introducing additional significant errors in the calculated rates of the dominant non-CNO reactions [see the fifth column of Table XI for the calculated partial derivatives of neutrino fluxes with respect to the important cross-section factor for the reaction $^{14}\mathrm{N}(p,\gamma)^{15}\mathrm{O}$].

The most important cross-section factors are shown in Table III. We also give in this table the estimated 1σ errors for the cross-section factors.

B. The solar constant

Recent measurements of the solar constant show agreement with each other at the level of a percent. Willson, Duncan, and Geist (1980) obtained 1368.1 ± 0.5 W/m^2 and 1373.4 ± 0.5 W/m^2 from two separate rocket flights. Hickey *et al.* (1980) find an average value, using an instrument on the Nimbus 7 satellite, of 1376.0 ± 0.7 W/m^2. An earlier discussion by these authors, Willson and Hickey (1977), indicated a weighted average value for many measurements of 1370 ± 1 W/m^2. Most recently, Willson *et al.* (1981) find 1368.3 W/m^2 using 153 days of data from an instrument aboard the NASA Solar Maximum Mission Spacecraft. The systematic errors in some of the experiments appear to be larger than the statistical errors.

We adopt a nominal value and an uncertainty that is consistent with all of the above numbers, i.e., an average solar flux at 1 A.U. of 1372 ± 4 W/m^2 or

$$L_\odot = 3.86(1 \pm 0.005) \times 10^{33} \text{ erg/sec}. \tag{13}$$

C. Element abundances

Two assumptions regarding chemical composition are made in constructing a standard solar model. First, the sun is assumed to be chemically homogeneous when it arrives on the main sequence. Second, the composition of the present solar surface is assumed to reflect the initial abundances of all elements heavier than hydrogen and helium. The justifications for these assumptions (and some of the consequences of their violation in nonstandard models) are given in several of the review articles cited in the first paragraph of Sec. II.

Table IV shows the number abundances (and uncertainties) with respect to hydrogen ($\log_{10} N = 12$ for hydrogen) recommended by several different authors using a variety of criteria and techniques, which sometimes overlap and sometimes are different. The reader is urged to consult the original papers referred to in Table IV in order to appreciate the detailed analyses that are responsible for each of the numbers given. [The fifth column refers to papers by Lambert (1978) and Lambert and Luck (1978); the series of Lambert-Warner analyses is referenced in Lambert and Warner (1968) and Bahcall and Ulrich (1971).]

Many matters of judgment enter the determination of a "solar abundance" (see, for example, the discussions by Withbro, 1971; Pagel, 1973; Meyer, 1979). Some of the more important factors include the choice of spectroscopic lines, the choice of atomic data (f values), the use of particular solar atmospheric models, the theory of line formation adopted, and the weight attached to meteoritic determinations.

TABLE IV. Comparison of some recent abundance determinations. The numerical entries are the logarithms of the number abundances, normalized to $\log N = 12$ for hydrogen.

Species	Cameron (1981)	Hauge and Engvold (1977)	Holweger (1979)	Lambert (1978)	Lambert-Warner (Bahcall and Ulrich, 1971)	Ross-Aller (1976)
C	8.62	8.4	8.50	8.67±0.1	8.55	8.62±0.12
N	7.94	7.9	7.93	7.99±0.1	7.93	7.94±0.15
O	8.84	8.8	8.82	8.92±0.1	8.77	8.84±0.07
Ne	7.99	7.7	7.74		7.88	7.57±0.12
Mg	7.60	7.6	7.57	7.62	7.48	7.60±0.15
Si	7.57	7.5	7.60	7.63	7.55	7.65±0.08
S	7.27	7.2	7.19	7.23	7.28	7.2 ±0.15
Fe	7.53	7.6	7.52		7.56	7.50±0.08

Table IV gives an indication of the spread in abundance values that are current. However, the individual values are not all independent, and unknown systematic errors (and overlapping techniques) may affect similarly all of the cited abundance determinations for a given element. Hence the agreement among the tabulated values is not necessarily a measure of the absolute uncertainties.

For specificity, we adopt the Ross-Aller (1976) relative metal abundances as our standard values. Prior to 1980, papers on the solar neutrino problem in the present series used the Lambert-Warner abundances that are tabulated in the sixth column of Table IV. The logarithmic differences (generally less than ± 0.1) between the Ross-Aller and the Lambert-Warner abundances are a useful guide to what changes are possible in a decade.

Two ways of estimating the fractional uncertainty in Z, the mass fraction of all elements heavier than helium, are discussed below. Neither of these methods is very reliable, but both give approximately the same answer. The spread in the values of Z calculated from the different abundance estimates given by experts and cited in Table IV is

$$\Delta Z/Z = 0.1. \tag{14}$$

The uncertainties quoted by Ross and Aller for individual elements (see Table IV) can be combined to yield an estimated total uncertainty if the uncertainties are assumed uncorrelated. This estimate yields $\Delta Z/Z = 0.1$, in agreement with Eq. (14).

Oxygen provides the largest single contribution ($\approx 50\%$) to the estimated total heavy element abundance. Fortunately, Lambert (1978) has provided an extensive analysis of the major ingredients that enter importantly the determination of the photospheric abundances of carbon, nitrogen, and oxygen (which together constitute about 75% of the standard total heavy element abundance).

Lambert (1981) has performed a detailed evaluation of the approximate 3σ error for the solar photospheric abundance of oxygen based on the results given in Lambert (1978). We are indebted to Professor Lambert for generously permitting us to summarize his conclusions below.

The main uncertainties that enter the oxygen determinations are (1) the spread in values given by different model atmospheres, (2) the uncertainty in the absolute f values, (3) the measured equivalent widths, and (4) questions about the applicability of the standard assumptions. Lambert (1981) concentrates on the magnetic dipole transitions of [OI] at 6300 and 6363 Å. These lines have the best-determined f values, and the NLTE effects are relatively unimportant for them.

The spread among the four most reliable model atmospheres (denoted HM, VAL, AL, and A) used in constructing Table 6 of Lambert (1978) was 0.04 dex, suggesting a model-atmosphere uncertainty of about ± 0.02 dex. The gf-values of the magnetic dipole transitions are known to at least ± 0.02 dex as a result of Garstang's calculations that were reported by Lambert (1978). Lambert (1981) estimates that the equivalent widths of the two [OI] lines are known independently to $\pm$ 5%, as a result of a reinspection of the Liège Atlas. The major source of systematic error is likely to be the continuum placement. However, the two lines give the same abundance to an accuracy of ± 0.03 dex, which suggests that systematic errors are small. The 6363 Å line has two weak blends; 6300 Å appears to be free of blends. For the two magnetic dipole lines considered here, LTE is expected to be an excellent approximation.

Assuming that the errors mentioned above are independent, Lambert (1981) estimates an overall uncertainty in the oxygen abundance of $\pm$ 9%, which also is consistent with Eq. (14).

In what follows, we assume that the total heavy element abundance is known to an accuracy of 10%.

D. Rosseland mean opacity

The neutrino fluxes calculated with the aid of solar models depend upon the Rosseland mean opacities adopted for the solar interior. The opacity depends upon the chemical composition and on the modeling of complex atomic processes. Opacity calculations are difficult to carry out for the conditions in the solar interior and constitute a major source of uncertainty for solar neutrino calculations (see Huebner, 1978).

Only a few opacity computer programs can handle complex astrophysical mixtures, but several programs have been available to make comparisons of opacity for individual elements or for very simple mixtures in overlapping regions of density and temperature. Various independent comparisons have been made using Los Alamos opacity programs based on different atomic physics models and the Los Alamos Astrophysical Opacity Library (Huebner, Merts, Magee, and Argo, 1977) as standards. In the comparisons, most disagreements have been traced and explained. Results from Los Alamos codes, based on the screening constant (scaled Hartree-Fock) model of the atom on one hand, and based on the Thomas-Fermi model on the other hand, have also been compared with each other and with the Astrophysical Opacity Library; they are found to be in good agreement. For a comparison between Los Alamos and Livermore codes, see below.

A comparison has also been made with the opacities calculated by T. R. Carson (1976) for a stellar mixture ($X = 0.73$, $Z = 0.02$) which is similar to, but not the same as, the solar mixture adopted here. Carson considers fourteen metals in his mixture, but the abundances for two of these (Cr and Ni) were combined with that for Fe. Thus the lines and photoelectric edges of Cr and Ni will coincide with those of Fe and will not be as effective in blocking radiation. His adopted relative abundance of the metals is close to that compiled by Cameron (1973), which has a much higher abundance for Ne (close to that of N), a lower abundance for the iron-like metals, and other variations, relative to Ross and Aller (1976). Since Carson's opacities are on a different

temperature-density grid than our opacities, a comparison was made only at a few temperatures close to our grid. Only a density interpolation was required; it is more reliable than a temperature interpolation. Following the density-temperature track of the sun, Carson's opacities are 33% smaller than the LASL values at 10^6 K, at 10^7 K they are 8% smaller, and at about 15.7×10^6 K they are $\sim$ 17% smaller. It should be noted that the often referred to, but unexplained, C-N-O bump in Carson's opacities occurs at $\sim 10^6$ K but at much lower densities than are important here. But the bump casts a general suspicion on his tables.

Special opacity tables from the Los Alamos Astrophysical Opacity Library (Huebner, Merts, Magee, and Argo, 1977) were prepared for use in the present calculations. These tables follow the run of temperature and density in the sun.

The opacities used in standard models in the previous decade (for example, Bahcall *et al.*, 1973) and those for the new model (cf. Bahcall *et al.*, 1980) are compared in Table V. Note that the new opacities are typically 15–20% larger than the old opacities near the center of the sun, 7×10^6 K $< T < 16\times10^6$ K, where the influence on neutrino fluxes is greatest (see Bahcall, Bahcall, and Ulrich, 1969, Fig. 2).

The differences between the old and new opacities are due mainly to improvements in the calculations of the physical processes that determine the opacity rather than in the assumed solar compositions. This conclusion was established in the following way. An opacity table was prepared for the same composition as was adopted in the old Lambert-Warner opacity set (Bahcall and Ulrich, 1971), but the code for performing the opacity calculation was the same as was used for the new opacities. This opacity table is also given in Table V, where it is labeled "new code, old composition." Notice that this hybrid is much closer to the new opacities than the old opacities. The change in total metal abundance Z and in the relative abundances among the metals contribute only 4% to the 20% increase mentioned above. We conclude that changes in the treatment of physical processes within the opacity code, rather than changes in chemical composition, are responsible for the differences between the old and new opacity tables.

The principal changes in the Los Alamos code have been the replacement of hydrogenic photoelectric cross sections by nonhydrogenic cross sections (which include multipole and relativistic effects that begin to contribute at the center of the sun), a better treatment of line wings, and the inclusion of a large number of weak absorption lines, many of them in the spectral regions that previously had a low extinction (Magee, Merts, and Huebner, 1975).

Also shown in the last column of Table V are the opacities that were calculated with no metals, $X = 0.75$, $Y = 0.25$. Here X and Y are the mass fractions, respectively, of hydrogen and helium. By comparing the last three columns of Table V, we see that more than half of the radiative opacity in the central regions ($T > 10^7$ K) of the sun is produced by photon scattering on free electrons and by inverse bremsstrahlung in the presence of completely ionized hydrogen and helium, processes that can be calculated with an accuracy of better than 10%.

The accuracy of the new Los Alamos opacity was checked by comparing it with a table computed by an independent code developed at Livermore (Rosznyai, 1980).

TABLE V. Comparison of Rosseland mean opacity from old and new codes with old (Lambert-Warner) and new (Ross-Aller) composition.

	T (K)	ρ (g cm^{-3})	Old code Old composition ($X=0.7877, Z=0.0163$) κ (cm^2 g^{-1})	New code New composition ($X=0.75, Z=0.0179$) κ (cm^2 g^{-1})	New code Old composition ($X=0.7877, Z=0.0163$) κ (cm^2 g^{-1})	New code ($X=0.75, Y=0.25$) κ (cm^2 g^{-1})
$\rho/T_6^3=0.035$	15.7×10^6	135.0	1.23	1.41	1.41	0.829
	12.8	73.4	1.36	1.58	1.56	0.890
	11.3	50.5	1.46	1.71	1.67	0.931
	10.0	35.0	1.56	1.89	1.82	0.973
	7.0	12.0	2.22	2.91	2.76	1.11
	4.5	3.19	4.91	6.51	6.18	1.32
	3.0	0.945	11.5	14.8	14.5	1.69
	1.8	0.204	30.3	34.1	31.8	2.35
	1.0	0.035	49.1	52.4	46.4	4.42
$\rho/T_6^3=0.041$	15.7×10^6	159.0	1.30	1.50	1.50	0.887
	12.8	86.0	1.45	1.70	1.68	0.953
	11.3	59.2	1.54	1.84	1.79	0.998
	10.0	41.0	1.66	2.02	1.95	1.05
	7.0	14.1	2.33	3.10	2.95	1.20
	4.5	3.74	5.10	6.90	6.54	1.45
	3.0	1.11	12.1	15.6	15.3	1.84
	1.8	0.239	33.0	37.6	35.2	2.62
	1.0	0.041	53.4	57.7	51.2	4.97

There are fundamental differences between the two codes. The Los Alamos code is based on the explicit ion model (also known as the method of detailed configuration accounting) at densities below ~ 1 g cm^{-3} and temperatures below 100 eV. This method requires the calculation of all possible ionization stages and all singly and multiply excited states for each ion. Outside this region, a mean ion model based on screening constants is used. For a more detailed description of these models, see Huebner (1982). On the other hand, the Livermore code uses, for all temperatures and densities, a mean ion model based on relativistic Hartree-Fock-Slater calculations. Further, the Los Alamos code makes use of photoelectric cross sections normalized to measured values and determines spectral line and photoelectric edge positions from laboratory data of atomic energy levels, while the Livermore code calculates these quantities consistent with the assumed atomic model.

The opacity tables generated by the Livermore (LLL) code are shown in Table VI. Notice that the Livermore opacities are generally smaller by no more than 10% than the Los Alamos (LASL) opacities, except at the lowest temperatures (which are not important for our purposes), where they are actually larger than the LASL values. Part of the systematic deviation at high temperatures can be explained by the more limited capability of the Livermore code, which can process only ten elements in a mixture (although the abundances of some neighboring elements had been combined in their calculations) versus twenty elements considered in detail in the Los

TABLE VI. Comparison of Los Alamos and Livermore solar opacities κ (cm^2 g^{-1}) with Ross and Aller (1976) metal abundances ($Z=0.0179$).

		T (K)	ρ (g cm^{-3})	LASL κ	LLL κ	%
$\rho/T_6^3=0.035$	$X=0.75$	15.7×10^6	135.0	1.405	1.352	−3.7
		12.8	73.4	1.583	1.495	−5.6
		11.3	50.5	1.712	1.576	−7.9
		10.0	35.0	1.888	1.738	−7.9
		7.0	12.0	2.914	2.693	−7.6
		4.5	3.19	6.509	6.427	−1.3
		3.0	0.945	14.77	14.38	−2.6
		1.8	0.204	34.08	37.48	10
		1.0	0.035	52.35	64.54	23
	$X=0.35$	15.7×10^6	135.0	1.183	1.101	−6.9
		12.8	73.4	1.337	1.183	−11.5
		11.3	50.5	1.453	1.317	−9.4
		10.0	35.0	1.608	1.461	−9.1
		7.0	12.0	2.537	2.329	−8.2
		4.5	3.19	5.852	5.831	−0.4
		3.0	0.945	13.58	13.29	−2.1
		1.8	0.204	31.01	37.45	21
		1.0	0.035	49.92	60.39	21
$\rho/T_6^3=0.041$	$X=0.75$	15.7×10^6	159.0	1.497	1.429	−4.5
		12.8	86.0	1.696	1.618	−4.6
		11.3	59.2	1.836	1.683	−8.3
		10.0	41.0	2.023	1.863	−7.9
		7.0	14.1	3.104	2.884	−7.1
		4.5	3.74	6.897	6.768	−1.9
		3.0	1.11	15.64	15.30	−2.2
		1.8	0.239	37.60	41.37	10
		1.0	0.041	57.65	70.60	22
	$X=0.35$	15.7×10^6	159.0	1.264	1.167	−7.7
		12.8	86.0	1.434	1.317	−8.2
		11.3	59.2	1.559	1.390	−11
		10.0	41.0	1.725	1.555	−9.9
		7.0	14.1	2.712	2.452	−9.6
		4.5	3.74	6.210	6.183	−0.4
		3.0	1.11	14.47	13.99	−3.3
		1.8	0.239	34.12	41.70	22
		1.0	0.041	55.31	70.71	28

Alamos results. The opposite deviation at the low temperatures stems from the detailed line treatment in the Los Alamos codes versus smeared line approximation in the Livermore code. These opacities are given for $Z = 0.0179$.

Not included in Tables V and VI are corrections for collective effects on scattering. These effects lower the opacity in the sun's center by about 5%. In the calculations reported here we have used the results by Diesendorf (1970), which indicate that the cross section for photon scattering by electrons is decreased by about 35% for the typical temperatures and densities of a solar model. Since the scattering cross section is nearly gray, we have reduced the total opacity by $0.07\,(1 + X)$ cm^2/g throughout the solar model. Formulas given by Huebner (1982) indicate that this correction overestimates the change by about 1% in the total opacity, i.e., the opacity we used is about 1% too low.

At the center of the sun, the opacity, in all the mixtures discussed, is dominated by inverse bremsstrahlung.

E. The equation of state

In earlier papers in this series, we used a conventional equation of state that includes radiation pressure and also screening interactions according to the Debye-Hückel theory (see references in the caption of Fig. 4 for details). We assumed that the solar plasma is completely ionized for all temperatures above 10^5 K (i.e., everywhere except in the surface layers). However, the study by Bahcall, Bahcall, and Ulrich (1969) showed that the calculated neutrino flux from ^{8}B decay is sensitive to local changes in the equation of state. Recently, Ulrich (1982) has derived a somewhat improved equation of state that does not make the *ab initio* assumption of full ionization in the solar interior. This equation of state takes account of scattering states according to the prescriptions of Larkin (1960), Ebeling, Kraft, and Kremp (1977), and Ebeling and Sandig (1973). We compare in Sec. IV the small differences in solar neutrino fluxes calculated using the standard and the improved equation of state. These differences are the only available measures of how large might be the uncertainties in neutrino fluxes caused by uncertainties in the equation of state.

F. The solar age

The age of the meteorites is accurately determined and is about 4.55×10^9 yr (see, for example, Wasserburg *et al.*, 1977, 1980). The time interval between the formation of the meteorites and the formation of the sun is uncertain, but is expected by most workers to be small on the time scales of interest here. Moreover, the precise age of the sun is not important for our purposes as long as it is in the currently believed range ($\sim 4.6 \pm 0.1 \times 10^9$ yr).

III. STANDARD MODELS

A. General method

Evolutionary sequences of the sun were constructed beginning with a zero-age main sequence model with a homogeneous composition. Successive models were calculated by allowing for composition changes caused by nuclear reactions. The models were constructed by integrating from the center outward and from the surface inward, requiring that the two solutions match at a convenient point. Some details of the code and the calculational procedures are described by Bahcall and Ulrich (1971) and in Appendices A and B of the present paper. Bahcall and Sears (1972) described and compared many of the earlier standard models.

The standard parameters were taken from the best-estimate values given in Sec. II. The equation of state included Debye-Hückel and degeneracy corrections, as well as radiation pressure. Convenient tables of specially constructed Los Alamos opacities were used (see Tables V and VI), which were designed to bracket the solar interior conditions so that complicated interpolations would not be necessary. These tables were constructed for an elemental mixture with $Z = 0.0179$ and two values of X, so that the model interpolates the opacity table in X. The ratios of heavy element abundances were taken from Ross and Aller (1976).

A primordial value of X, the initial homogeneous hydrogen abundance, and S, the entropylike variable discussed in Appendix A which defines the adiabat of the convection zone, were chosen and a series of (usually 5) solar models were constructed. An eigenvalue solution with a luminosity equal to $L_\odot$ and radius $R_\odot$ at an elapsed time of 4.7×10^9 yr was sought. The initially assumed values of X and S were iterated until an eigenvalue was obtained. The empirical relations used as guides in this iterative process were

$$\frac{\Delta X}{X} = -0.152\frac{\Delta L}{L} - 0.064\frac{\Delta R}{R}, \tag{15a}$$

and

$$\frac{\Delta S}{S} = -0.366\frac{\Delta L}{L} + 1.40\frac{\Delta R}{R}, \tag{15b}$$

where R is the computed solar radius, and L is the calculated total luminosity (including positive contributions from the p-p and CNO reactions as well as the negative contribution from gravitational expansion). Here, for example, ΔX is $X_{(\text{desired})} - X_{(\text{previous})}$. For typical cases, the calculated model luminosity and radius were equal to the observed solar values to a fractional accuracy of better than 0.001 after three iterations (sequences of models). For the standard model, the value of S corresponds roughly to $l/H = 1.8$.

The solution determines the primordial values of X, Y, Z, the present complete run of physical variables inside the convection zone, and, of course, the neutrino fluxes.

The value of Z/X, rather than Z, is most directly

determined from observations. Ross and Aller (1976) deduced $Z/X = 0.0228$ for the surface abundances of the sun. A final step in obtaining the calculated neutrino fluxes involves a correction for the Z/X value obtained from the solar model to the Z/X value given by Ross and Aller. This correction is easily made with the aid of the derivatives $\partial \ln\phi_i / \partial \ln(Z/X)$ which are given in the next to the last column of Table XI.

All previous papers in this series have used the same basic procedures and give many of the details necessary for the calculations (for references, see the caption of Fig. 4). The crude treatment of the atmosphere used for the present paper is described in Appendix A and the procedure used to integrate the nuclear abundance equations is outlined in Appendix B.

B. Some characteristics of the standard model

We give in Table VII the run of the physical variables in our standard solar model. The quantities tabulated include mass fraction, fraction of the solar radius, temperature, density, hydrogen abundance, luminosity fraction, and representative neutrino fluxes. The relation between density ρ (in $\mathrm{g\,cm^{-3}}$) and temperature T_6 (in units of 10^6 K), is given approximately by

$$\rho = 0.042\ T_6^3 \tag{16}$$

for $T_6 > 6$.

There are a number of characteristics of the standard model that are of general interest. For example, the fraction of the luminosity that originates in the *p-p* chain is 0.985; the corresponding fraction for the CNO cycle is 0.015. The gravitational expansion at the present epoch corresponds to a luminosity fraction of -0.0003. The convection zone terminates at 2.0×10^6 K, corresponding to a radius of $0.73 R_\odot$ and a density of $0.15\ \mathrm{g\,cm^{-3}}$. With regard to the distribution within the sun, one-half of the luminosity (or flux of neutrinos from the *p-p* reaction) is produced within the inner $0.09\ M_\odot$ ($R \leq 0.1 R_\odot$); the corresponding number for 95% production is $0.35 M_\odot (R \leq 0.2 R_\odot)$. For the flux of neutrinos from ^{8}B decay, 95% is produced within the inner $0.05\ M_\odot (R \leq 0.08 R_\odot)$.

The second column of Table VIII gives the total computed neutrino fluxes for each of the important neutrino sources that are obtained with the standard parameters of Sec. II. The small differences between the values given here and those obtained earlier by Bahcall *et al.* (1980) are caused mainly by the slightly improved values for the CNO cross-section factors (see Table III) and the somewhat lower (by $\sim$ 6%) value for $S_{17}(0)$ [see the discussion of the ^{7}Li$(d,p)^8$Li cross section in Sec. II.A.7, two paragraphs before Eq. (12)] that were used in the present calculations.

The neutrino energy spectrum that corresponds to the standard fluxes of Table VIII is shown in Fig. 2.

Table IX presents the computed solar luminosity and radius as a function of time. The model of the present sun has a luminosity that has increased by 44% from the nominal (see below) zero-age model and the effective temperature has increased by 2%. The zero-age model in our sequence is homogeneous. Because ^{3}He and the CNO elements have their initial values, this model is actually on a ^{3}He main sequence (Ulrich, 1971) and has a lower luminosity than it will have on the normal main sequence. The model at 0.5×10^9 yr is largely beyond the initial transient (see Appendix B for a discussion of the numerical method of calculating the approach to steady-state abundances). The first row in Table IX refers to nominal zero-age values obtained by extrapolating backwards from the model at 0.5×10^9 yr.

C. The primordial helium and oxygen abundances

The primordial helium abundance, Y, is determined in our standard models by the requirement that at the age of the sun the models must have the observed values for the solar luminosity, mass, radius, surface composition, and (Z/X). For the model given in Table VII, $Y = 0.250$ and the primordial value for $(Z/X) = 0.024\,57$. By constructing a series of solar models with opacity tables calculated with different values for the primordial heavy element abundance, we have evaluated the logarithmic derivative of Y with respect to (Z/X). The result is given in the first row of Table X. Using this derivative, we obtain a value for the primordial helium abundance of $Y = 0.244$ for a model that would have Ross-Aller value, $Z/X = 0.0228$, for the primordial heavy element to hydrogen ratio. The standard model calculated with the aid of the improved equation of state discussed by Ulrich (1982) (see also Sec. II.E) yields a primordial helium abundance of $Y = 0.252$ for the Ross-Aller value of Z/X. These results can be compared to the helium to hydrogen abundance ratio of $N_{\mathrm{He}}/N_{\mathrm{H}} = 0.095$ to 0.11 found by Leckrone (1971) for hot stars and by Peimbert and Torres-Peimbert (1977) for the Orion nebula. Using the Ross-Aller value of Z/X these numbers translate to $0.27 < Y < 0.30$.

The sensitivity of the inferred primordial helium abundance to changes in input parameters is given in Table X, where the logarithmic derivatives of Y with respect to the assumed solar age, the solar luminosity, and the most important nuclear parameters are listed. These derivatives were calculated with the aid of a series of standard solar models.

The last column of Table X gives the fractional uncertainties in the primordial helium abundances of the standard solar model that result from the recognized uncertainties in input parameters that were discussed in Sec. II. The largest listed contribution to the uncertainty in the inferred helium abundance is caused by the uncertainty in the primordial value of Z/X and is of order a few percent.

We conclude that standard solar models yield a well defined value for the primordial helium abundance:

$$Y = 0.25 \pm 0.01. \tag{17}$$

The primordial oxygen abundance that we have as-

TABLE VII. Standard solar model.

$M(r)/M_\odot$	$r/R_\odot$	T (10^6 K)	ρ (g cm^{-3})	$X(^1\mathrm{H})$	$X(^3\mathrm{He})$	$L_i(r)/L_\odot$	$\phi_i(pp)$ (Fractional)	$\phi_i(^7\mathrm{Be})$ (Fractional)	$\phi_i(^8\mathrm{B})$ (Fractional)
0.0000	0.0000	15.50	156.3	0.3545	8.94E-06				
0.0008	0.0197	15.36	151.7	0.3663	9.90E-06	0.0067	0.0049	0.0241	0.0570
0.0099	0.0462	14.81	133.9	0.4171	1.52E-05	0.0722	0.0579	0.2224	0.4136
0.0385	0.0759	13.84	108.1	0.4965	2.93E-05	0.1849	0.1683	0.3812	0.4080
0.0731	0.0977	13.01	90.20	0.5550	4.95E-05	0.1717	0.1703	0.1986	0.0955
0.1038	0.1131	12.41	78.86	0.5922	7.22E-05	0.1191	0.1229	0.0815	0.0187
0.1346	0.1267	11.88	69.90	0.6209	1.01E-04	0.0950	0.0997	0.0420	0.0051
0.1620	0.1378	11.45	63.24	0.6412	1.33E-04	0.0683	0.0723	0.0205	0.0014
0.1860	0.1469	11.10	58.13	0.6559	1.66E-04	0.0496	0.0527	0.0108	0.0004
0.2100	0.1558	10.78	53.57	0.6684	2.07E-04	0.0416	0.0442	0.0068	0.0002
0.2340	0.1643	10.47	49.44	0.6788	2.55E-04	0.0347	0.0387	0.0044	0.0001
0.2580	0.1727	10.19	45.68	0.6876	3.12E-04	0.0300	0.0310	0.0028	0.0000
0.2820	0.1809	9.911	42.20	0.6951	3.81E-04	0.0242	0.0258	0.0018	0.0000
0.3100	0.1904	9.600	38.48	0.7023	4.81E-04	0.0230	0.0246	0.0013	0.0000
0.3500	0.2038	9.174	33.69	0.7104	6.71E-04	0.0251	0.0269	0.0010	0.0000
0.3900	0.2173	8.767	29.41	0.7164	9.39E-04	0.0180	0.0193	0.0005	0.0000
0.4300	0.2309	8.374	25.57	0.7208	1.33E-03	0.0128	0.0137	0.0002	0.0000
0.4700	0.2449	7.995	22.09	0.7239	1.89E-03	0.0090	0.0095	0.0001	0.0000
0.5100	0.2593	7.626	18.93	0.7261	2.62E-03	0.0062	0.0066	0.0000	0.0000
0.5500	0.2745	7.266	16.06	0.7276	3.22E-03	0.0038	0.0044	0.0000	0.0000
0.6900	0.3364	6.028	8.030	0.7312	1.12E-03	0.0038	0.0062	0.0000	0.0000
0.8300	0.4297	4.653	2.846	0.7321	1.85E-04	0.0003	0.0001	0.0000	0.0000
0.9264	0.5545	3.403	0.7727	0.7322	1.03E-04	0.0000	0.0000	0.0000	0.0000
0.9602	0.6409	2.718	0.3381	0.7322	1.00E-04	0.0000	0.0000	0.0000	0.0000
0.9784	0.7184	2.120	0.1689	0.7322	1.00E-04	0.0000	0.0000	0.0000	0.0000
0.9954	0.8492	0.9499	0.0496	0.7322	1.00E-04	0.0000	0.0000	0.0000	0.0000
1.000	1.000	0.0058	0.0000	0.7322	1.00E-04	0.0000	0.0000	0.0000	0.0000

TABLE VIII. Neutrino fluxes for solar models with differing nuclear cross sections. Here $EXY = 10^{xy}$.

Model Source	Standard	$S_{34}=0.61$ keV b	$S_{34}=0.30$ keV b	$S_{33}=5.1$ keV b
p-p	6.07*E*10	6.02*E*10	6.23*E*10	6.10*E*10
pep	1.50*E*8	1.48*E*8	1.55*E*8	1.50*E*8
^{7}Be	4.3*E*9	4.95*E*9	2.6*E*9	4.15*E*9
^{8}B	5.6*E*6	6.4*E*6	3.45*E*6	5.4*E*6
^{13}N	5.0*E*8	4.9*E*8	5.1*E*8	5.0*E*8
^{15}O	4.0*E*8	4.0*E*8	4.1*E*8	4.0*E*8

sumed for the standard solar model is sufficiently large, $X(16) = 0.008\,74$, that the calculated neutrino flux from ^{17}F is due almost entirely to the reaction $^{16}\mathrm{O}(p,\gamma)^{17}\mathrm{F}$ on primordial oxygen. This result is of interest since the primordial abundance of heavy elements in the central region of the sun has been assumed to be inaccessible to observation although it is of great importance in constructing non-standard (so-called low-Z) models of the sun (see for example, Bahcall and Ulrich, 1971). We find for the standard solar model

$$\phi(^{17}\mathrm{F}) = 5\times10^{6}\ \mathrm{cm}^{-2}\mathrm{sec}^{-1}\ , \tag{18}$$

a value that is about equal to the flux of solar neutrinos from the decay of ^{8}B. However, the product of flux times neutrino absorption cross section for ^{17}F is too small to give a measurable effect in any of the proposed experiments. We find, for example, that $\sigma(^{17}\mathrm{F}) = 6.65\times10^{-46}$ cm^2 for ^{37}Cl and $\sigma(^{17}\mathrm{F}) = 92.4\times10^{-46}$ cm^2 for ^{71}Ga. (For the procedures used to obtain these values, see Bahcall, 1978.) The expected neutrino capture rate from ^{17}F is less than 0.05% for both the chlorine and gallium experiments.

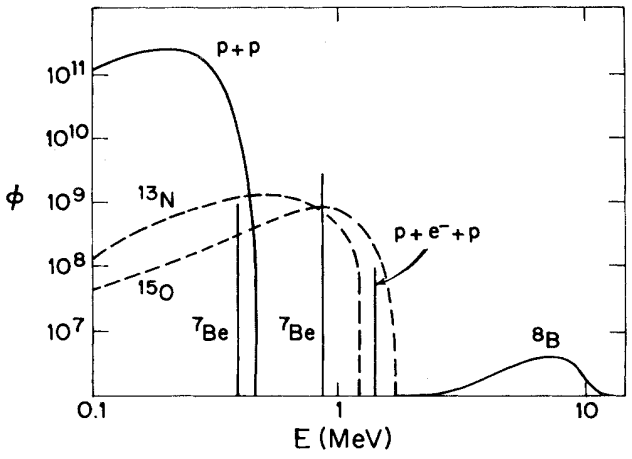

FIG. 2. The energy spectrum of solar neutrinos as predicted by the standard model. Solid lines: neutrinos from the *p-p* chain. Broken lines: neutrinos from the CNO cycle. Fluxes are in numbers cm^{-2}sec^{-1}MeV^{-1} for continuum sources and numbers cm^{-2}sec^{-1} for line sources.

D. Nonradial *p*-mode oscillations

The oscillation frequencies of the sun provide an important way of studying the structure of the sun, in much the same way as seismology enables us to learn about the structure of the Earth.

The solar *p*-mode (five-minute) oscillations have been observed in sufficient detail to determine both the dominant frequencies and the horizontal wavelengths (Leighton, 1961; Leighton, Noyes, and Simon, 1962; Deubner, 1975; Rhodes, Ulrich, and Simon, 1977; Claverie *et al.*, 1979; Deubner, Ulrich, and Rhodes, 1979; Grec, Fossat, and Pomerantz, 1980 and references contained therein). One important datum that is relevant to models of the solar interior is that the power in the five-minute range is resolved into many approximately equidistant peaks separated by 68 μHz. The splitting of these peaks, which is different for even and odd lines, indicates that global modes of oscillation with spherical harmonics of order $l = 0$, 1, 2, and 3 have been identified. Theoretical interpretations of the five-minute oscillation phenomena have been given by a number of authors (e.g., Ulrich, 1970; Leibacher and Stein, 1971; Iben and Mahaffy, 1976; Ulrich and Rhodes, 1977; Gough, 1978; Christensen-Dalsgaard and Gough, 1980; and Issak, 1980 and references cited therein).

The separation between the frequencies of adiabatic *p*-

TABLE IX. Solar luminosity and radius versus time.

Time (10^9 yr)	Radius (10^{10} cm)	Luminosity (10^{33} erg sec^{-1})	T_e (10^3 K)
0.000	6.07	2.68	5.65
0.525	6.17	2.81	5.67
1.575	6.32	3.03	5.71
3.155	6.60	3.40	5.75
4.735	6.96	3.86	5.78

TABLE X. The dependence of the inferred primordial helium abundance on various parameters.

Logarithmic derivative	Numerical value	Estimated contribution to the fractional uncertainty: $\Delta Y/Y$
$\frac{\partial \ln Y}{\partial \ln(Z/X)}$	-0.30	0.03
$\frac{\partial \ln Y}{\partial \ln(\text{Solar age})}$	-0.21	$\lesssim 0.01$
$\frac{\partial \ln Y}{\partial \ln L_\odot}$	$+0.4$	$\lesssim 0.01$
$\frac{\partial \ln Y}{\partial \ln S_{11}}$	$+0.1$	0.01
$\frac{\partial \ln Y}{\partial \ln S_{33}}$	$\lesssim 0.01$	< 0.01
$\frac{\partial \ln Y}{\partial \ln S_{34}}$	$\lesssim 0.01$	$\lesssim 0.01$

modes of low-degree l and high-order n is, for fixed n and $\Delta\ l\ = 2$ (Vandakurov, 1967; Tassoul, 1980; Christensen-Dalsgaard and Gough, 1980):

$$\Delta\nu_{n,l} \approx \left[2\int_0^R \frac{dr}{c} \right]^{-1}, \tag{19}$$

where c is the adiabatic sound speed.

The solar models discussed in this paper are rather crude in the region of the convective zone, which contains only the outer 2% of the solar mass (in twenty model zones) but which contributes about half of the p-mode splitting. We have therefore chosen to normalize our results for the fraction of the p-mode splitting that originates in various regions of the sun to the observed splitting of 136.0 μHz (Grec *et al.*, 1980). This normalization avoids the numerical inaccuracies inherent in our present treatment of the convective zone, but does not affect significantly the histograms discussed below.

The fractional contribution F to the p-mode splitting from any radial interval R to $R + \Delta R$ is

$$F = \frac{\int_R^{R+\Delta R} (dR/c)}{\int_0^{R_\odot} (dR/c)}. \tag{20}$$

The histogram of the fractional contributions to the observed p-mode splitting is shown in Fig. 3, which is taken from Bahcall (1981a), for mass fractions from 0.05 $M_\odot$ to $1.0M_\odot$, corresponding to radial intervals from $0.08R_\odot$ to $1.0R_\odot$. Also shown in Fig. 3 for comparison are the histogram for the production of neutrinos from ^{8}B decay and the histogram for the generation of the solar luminosity (which is nearly the same as the histogram for the production of neutrinos from the p-p reaction).

Figure 3 shows that the three observational quantities that are plotted are primarily determined in different regions. Nearly all of the neutrinos from ^{8}B decay originate in the inner 5% of the solar mass. Almost 70% of the p-mode splitting comes from the outer 10% of the solar mass. The generation of the solar luminosity, and the flux of neutrinos from the proton-proton reaction, are intermediate in distribution between the p-mode splitting and the flux of ^{8}B neutrinos. About 33% of the solar luminosity is produced in the inner $0.05M_\odot$ from which the neutrinos from ^{8}B decay also originate, but a

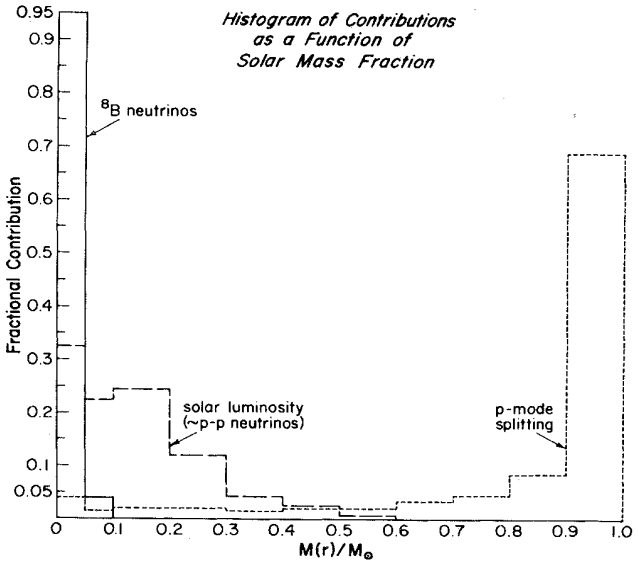

FIG. 3. Histogram of the fractional contributions to the p-mode splitting, the flux of neutrinos from ^{8}B decay, and the flux of neutrinos from the p-p reaction. Here $M(r)/M$ is the fraction of the solar mass interior to the point r. This figure is taken from the earlier discussion of Bahcall (1981a).

majority of the nuclear energy is produced in the intermediate region between $0.05M_\odot$ and $0.4M_\odot$.

The fractional decomposition shown in Fig. 3 is essentially independent of any plausible changes in nuclear cross sections. We have established this conclusion by deriving a model for the present-day sun using nuclear physics parameters that were all changed simultaneously to their 3σ limits (see Sec. II), each in the direction to reduce the flux of ^{8}B neutrinos (see Sec. IV.A for a list of the parameters used). For all three of the quantities shown in Fig. 3, the height of the histograms are the same to within ± 0.01 for the standard model and the one calculated with the extreme nuclear physics parameters.

The difference in the interior contribution, $0 \leq R \leq 0.9R_\odot$, between the values calculated for the splitting fraction F using the standard nuclear physics parameters and using the extreme nuclear physics parameters is about one percent, with the extreme model having the slightly larger interior contribution.

IV. UNCERTAINTIES IN THE CALCULATED NEUTRINO FLUXES

In this section we summarize the changes in calculated neutrino fluxes that result from small fractional changes in the important parameters that were discussed in Sec. II. We have evaluated the partial derivatives of the individual neutrino fluxes with respect to each of the parameters using standard solar models that were constructed with all but one (the quantity of interest) of the input parameters held fixed at their best-estimate values. The tabulated partial derivatives were calculated from the following relation:

$$\frac{\partial \ln\phi}{\partial \ln P} \equiv \frac{\ln(\phi_1/\phi_2)}{\ln(P_1/P_2)}\,, \tag{21}$$

where ϕ_1 and P_1 were, respectively, the standard values of the neutrino flux and the parameter and ϕ_2, P_2 were neighboring values [typically $(P_1-P_2)/P_1 \sim \pm 0.1$].

Comparisons are made with earlier determinations of the partial derivatives in order to show that the computed fractional changes do not depend very strongly on the adopted standard model.

We have evaluated also neutrino fluxes from solar models constructed with values for the ^{3}He$(\alpha,\gamma)^7$Be reaction rate that differ by a factor of 2, in order to evaluate the possible importance of a large deviation from the currently accepted cross-section factor for this reaction.

A. Effects of uncertainties in nuclear parameters

The partial derivatives of the individual neutrino fluxes with respect to the low-energy cross-section factors S_{11}, S_{33}, S_{34}, and S_{114} are given in columns two through five of Table XI (see Sec. II.A for a discussion of these parameters). Fractional changes in cross-section factors that were typically of order 10% were used for the numerical calculations of the tabulated partial derivatives. We have not listed the calculated derivatives with respect to S_{17}, since the rarity of this reaction guarantees that the only derivative that is numerically significant is $\partial \ln\phi(^8\text{B})/\partial \ln S_{17} = 1.00$.

The results given in Table XI generally agree well with the values of partial derivatives that have been published from time to time in the various articles cited in the first part of Sec. II. The dominant dependences are in excellent agreement (differences of ≤ 0.1 in logarithmic derivatives) with the values from Eq. (8) of Bahcall, Bahcall, and Ulrich (1969), which has been the most often used guide over the past decade to the sensitivities of solar neutrino fluxes.

The partial derivatives with respect to S_{114}, the cross section factor for the reaction $^{14}\text{N}(p,\gamma)^{15}\text{O}$, are given here for the first time, so far as we know.

We have verified that large changes in nuclear cross-section factors may be described reasonably accurately by the logarithmic derivatives given in Table XI. We have established this conclusion by calculating the eigenvalue neutrino fluxes when 3σ changes were made in nuclear cross-section factors. The results are shown in columns three through five of Table VIII. The reader may easily check that the fractional derivatives calculated for the large changes considered in Table VIII are in good agreement with the differential results of Table XI. The reason for this simple behavior is that the dependences of the most important neutrino fluxes on cross-section factors are basically power laws in the region of interest, as may be seen easily by writing out the form of the dependence of each flux on cross-section factors.

The fluxes given in the fourth column of Table VIII were obtained using the Munster value (Krawinkel *et al.*

TABLE XI. Some calculated partial derivatives of neutrino fluxes.

Source	$\frac{\partial \ln\phi_i}{\partial \ln S_{11}}$	$\frac{\partial \ln\phi_i}{\partial \ln S_{33}}$	$\frac{\partial \ln\phi_i}{\partial \ln S_{34}}$	$\frac{\partial \ln\phi_i}{\partial \ln S_{114}}$	$\frac{\partial \ln\phi_i}{\partial \ln L_\odot}$	$\frac{\partial \ln\phi_i}{\partial \ln Z}$	$\frac{\partial \ln\phi_i}{\partial \ln(Z/X)}$	$\frac{\partial \ln\phi_i}{\partial \ln(\text{Age})}$
p-p	+0.1	0.03	−0.06	−0.02	0.69	−0.06	−0.05	−0.07
^{7}Be	−1.0	−0.44	0.87	$\lesssim$0.01	3.5	0.68	0.60	1.1
^{8}B	−2.7	−0.42	0.83	$\lesssim$0.01	7.2	1.43	1.26	1.4
^{13}N	−2.4	−0.03	−0.10	0.85	5.8	1.90	1.67	1.15
^{15}O	−2.9	0.01	−0.03	1.00	6.8	2.27	2.00	1.45

1982), for $S_{34}(0) = 0.30$ keV b.

The tabulated partial derivatives can be used to obtain reasonably accurate estimates of the changes in the predicted neutrino fluxes even when all the nuclear physics parameters are simultaneously changed by large factors. We show in column two of Table XII the neutrino fluxes obtained with a solar model in which S_{11}, S_{33}, S_{34}, and S_{17} were all changed by amounts equal to their estimated 3σ limits (see Sec. II) in a direction that decreases the flux of ^{8}B neutrinos, i.e., $S_{11} = 4.23 \times 10^{-25}$ MeV b, $S_{33} = 5.5$ MeV b, $S_{34} = 0.37$ keV b, and $S_{17} = 0.019$ keV b. In column three, we give the neutrino fluxes calculated with the aid of Eq. (21) and the partial derivatives listed in Table XI. The agreement is excellent; in all cases the fluxes calculated by the two methods agree to better than or of order 8%.

B. Effects of uncertainties in the solar constant

The sixth column of Table XI contains the logarithmic partial derivatives of the neutrino fluxes with respect to the solar luminosity. These derivatives are useful in making small corrections to the fluxes calculated from solar models that do not have the precise solar luminosity, as well as for estimating the effect of uncertainties in the solar constant on the calculated fluxes.

The partial derivatives given here are similar to the results obtained by Bahcall, Bahcall and Ulrich (1969) with a rather different standard solar model. The derivatives calculated here for the *pep*, ^{7}Be, and ^{8}B fluxes agree with those determined earlier to better than 5%. The difference between old and new values is of order 20% for the ^{13}N flux, which was assumed equal to the ^{15}O flux in the 1969 models.

C. Effects of uncertainties in the total heavy element abundance

We have evaluated the sensitivity of the solar neutrino fluxes to the assumed total heavy element mass abundance Z, using specially prepared opacity tables. For this purpose, special opacity tables were calculated from the Los Alamos Astrophysical Opacity Library for different total values of Z but with fixed (Ross-Aller) relative abundances.

The logarithmic derivative of each neutrino flux was determined by evolving a series of solar models with different values of Z; for each value of Z, the model for the present sun was required to have the observed solar luminosity and radius.

The values for the logarithmic derivatives with respect to Z are shown in the seventh column of Table XI. The derivatives with respect to Z that are shown in Table XI agree in all cases with the previously determined values given by Bahcall and Ulrich (1971) to within an accuracy of 15%.

The iterations of the solar models are performed with respect to Z/X (see Sec. III.A) since this is the quantity that is determined by observations. Logarithmic derivatives of the individual fluxes with respect to Z/X are given in the next to last column of Table XI.

D. Effects of uncertainties in the individual heavy elements

Special opacity tables were calculated from the Los Alamos Astrophysical Opacity Library in which the abundances of carbon, nitrogen, oxygen, neon, magnesium, and iron were varied one at a time. A conventional series of standard solar models was constructed for each composition. The results permitted us to determine the sensitivity matrix A_{ij}, where

$$A_{ij} = \frac{\partial \ln \phi_i}{\partial \ln Z_j} \tag{22}$$

is the logarithmic derivative of the ith flux with respect to the abundance of the jth element. The derivatives computed for the flux of neutrinos from the decay of ^{8}B are close to the values given previously by Lubow *et al.* (1979).

The calculated values of A_{ij} are given in Table XIII for carbon, oxygen, neon, magnesium and iron. The calculated flux of neutrinos from ^{8}B decay depends most sensitively upon the assumed oxygen and iron abundances. The absolute values of the sensitivity matrix for the row pertaining to the proton-proton flux (and the *pep*

TABLE XII. Simultaneous 3σ changes in S_{11}, S_{33}, S_{34}, and S_{17}. The calculated neutrino fluxes were obtained for $S_{11}=4.23\times10^{-25}$ MeV b, $S_{33}=5.5$ MeV b, $S_{34}=0.37$ keV b, and $S_{17}=0.019$ keV b.

Source	Neutrino flux ($cm^{-2}sec^{-1}$) Solar model	Partial derivatives (see Table XI)	Fractional difference (in %)
p-p	6.25*E*10	6.27*E*10	0.5
pep	1.51*E*08	1.55*E*08	3
^{7}Be	2.72*E*09	2.52*E*09	7
^{8}B	2.05*E*06	2.22*E*06	8
^{13}N	3.75*E*08	3.61*E*08	4
^{15}O	2.80*E*08	2.64*E*08	6

TABLE XIII. Calculated dependence of fluxes on individual heavy elements.

Source $\frac{\partial \ln \phi_i}{\partial \ln Z_j}$	C	O	Ne	Mg	Fe
p-p	−0.008	−0.006	−0.001	−0.006	−0.014
^{7}Be	0.019	0.153	0.018	0.061	0.167
^{8}B	0.054	0.312	0.033	0.116	0.412
^{13}N	0.824	0.219	0.020	0.061	0.275
^{15}O	0.800	0.312	0.031	0.103	0.354

flux, not given) are all small, less than or of order 1%. The sensitivity to abundance changes in silicon and sulfur was not calculated. However, we expect, on the basis of general trends, that these two elements would yield partial derivatives of the same order as carbon and neon.

E. Opacities

The uncertainties that arise from calculated opacity values can be estimated by evaluating the neutrino fluxes for evolved solar models constructed with opacities from independent codes, holding all the other parameters constant. In Table XIV we give the individual neutrino fluxes that were obtained using both the Los Alamos Astrophysical Opacity Library and the Livermore opacity code (see Table VI for a direct comparison of the opacities), with the standard parameter values used in Bahcall *et al.* (1980) (which are similar to those adopted in this paper).

The computed fluxes from the *p-p*, *pep*, ^{7}Be, and ^{13}N reactions agree to better than 10%. The calculated fluxes from ^{8}B decay differ by about 16% and the fluxes from ^{15}O decay differ by about 11%.

The two opacity codes used in obtaining the fluxes given in Table XIV were written independently of each other; they also use different numerical and atomic-physics approximations. One is based on a combination of the explicit ion model (detailed configuration accounting) and a mean ion screening constant model, while the other code is based on a mean ion relativistic Hartree-Fock-Slater model. We believe that the spread of values given in Table XIV is indicative of the total plausible range of fluxes that can be obtained by using different state-of-the-art opacity codes with a fixed composition.

TABLE XIV. Neutrino fluxes calculated with Los Alamos and Livermore opacity codes for the standard model parameters of Bahcall *et al.* (1980).

Source	Los Alamos opacity (flux unit: 10^{10} cm^{-2}sec^{-1})	Livermore opacity
p-p	6.1	6.1
pep	0.015	0.016
^{7}Be	0.41	0.38
^{8}B	0.000 585	0.000 50
^{13}N	0.046	0.043
^{15}O	0.037	0.033

F. The equation of state

The neutrino fluxes calculated using the conventional and the improved equations of state that were described in Sec. II.E differ by less than or order of 1% for all the neutrino sources considered except for ^{15}O, for which the difference amounts to 1.5%. We conclude that recognized uncertainties in the equation of state are unimportant for predicting the solar neutrino fluxes.

G. The solar age

The logarithmic partial derivatives of the individual neutrino fluxes with respect to the assumed age of the sun are tabulated in the last column of Table XI. The uncertainties calculated from these derivatives are not important for our purposes if the age of the sun is known to $\pm 0.2 \times 10^{9}$ yr (cf. Sec. II.E).

The results given here are in reasonable agreement with, but are more accurate than, the dependence upon age calculated by Bahcall and Shaviv (1968) and Bahcall, Bahcall, and Ulrich (1969).

V. CAPTURE RATES FOR INDIVIDUAL NEUTRINO DETECTORS

A. General procedure

A number of possible detectors of solar neutrinos are being investigated actively with the goal of performing additional experiments. In this section we present the calculated 3σ uncertainties in the predicted capture rate, as well as a best-estimate rate, for each of the detectors for which we know about current experimental studies.

Our procedure is to combine incoherently the uncertainties that we estimate to exist in the predicted capture rates due to each of the factors discussed in Sec. II: individual nuclear rates, the solar constant, the primordial chemical composition, the solar radiative opacity, the equation of state, and the solar age, as well as the neutrino absorption cross sections. Let each of the solar neutrino fluxes be denoted by ϕ_i (e.g., *p-p* or ^{8}B neutrinos) and let each of the parameters be denoted by χ_j (e.g., S_{11}, $L_{\odot}$, or Z). Then we calculate a total incoherent uncertainty in the predicted rate, δR, by the relation

$$\delta R = \left[\sum_j \left[\sum_i (\phi_i \sigma_i)[(1 + d\chi_j/\chi_j)^{\alpha_{i,j}} - 1] \right]^2 \right]^{1/2}, \tag{23a}$$

$$\alpha_{i,j} = \frac{\partial \ln \phi_i}{\partial \ln \chi_j}. \tag{23b}$$

Here dX_j/X_j is the fractional uncertainty in any parameter X_j, and $\phi_i\sigma_i$ is the capture rate expected from neutrino flux ϕ_i. The neutrino fluxes, ϕ_i, are those calculated with the standard solar model and given in the second column of Table VIII. The neutrino absorption cross sections σ_i are taken from Bahcall (1978), except as noted otherwise. The best-estimate rate is $R \equiv \sum_i \phi_i\sigma_i$. We use in these numerical estimates the fractional uncertainties, dX_j/X_j, determined in Sec. II and the logarithmic derivatives of fluxes with respect to parameters that are given in Tables XI–XIV. For our purposes, it is a sufficient numerical approximation to assume that the logarithmic derivatives with respect to the *pep* flux are the same as the logarithmic derivatives of the *p-p* flux.

We estimate equivalent 3σ uncertainties based upon published data and calculations. Of necessity, we combine, via Eq. (23), uncertainties that result from measurement errors and those that result from calculational inadequacies. Judgment is required at all stages in this process; our particular choices are defined by the discussion in Sec. II. We use throughout this section the value and the uncertainty for the cross section factor for the ^{3}He-^{4}He reaction that is given in Eq. (8), although we note, where important, the results implied by the Munster value (see Krawinkel *et al.* 1982; Sec. II.A.5 of this paper, and the next to last column of Table VIII). For stellar opacities the fractional uncertainties in fluxes, $\Delta\phi_i/\phi_i$, are obtained from Table XIV by setting $\Delta\phi_i$ equal to one-half the difference in fluxes computed with the Los Alamos and Livermore opacities. The contribution to the total uncertainty represented by Eq. (23) that comes from the stellar opacity is $\sum_i \Delta\phi_i\sigma_i$.

The total fractional uncertainty in *individual* neutrino fluxes can be computed from the following expression:

$$\frac{\delta\phi}{\phi} = \left[\sum_j \left(\frac{\partial \ln\phi}{\partial \ln X_j}\right)^2 (dX_j/X_j)^2\right]^{1/2}. \quad (24)$$

The fractional uncertainties have been calculated using the logarithmic derivatives and fractional uncertainties in parameters described above and in Sec. II. Note that expressions (23) and (24) for the uncertainty in the total rate and in the individual fluxes are not proportional to each other when more than one neutrino flux contributes significantly to the expected capture rate.

Table XV lists the computed overall (effective 3σ) uncertainties in the individual neutrino fluxes that result from uncertainties in nuclear reaction rates, the solar constant, assumed primordial heavy element abundances, and stellar opacity. The fluxes of neutrinos from the decay of ^{8}B, ^{13}N, and ^{15}O are all uncertain by about 50%. The fractional uncertainty is 52% for the important flux of neutrinos from ^{8}B decay, with comparable uncertainties contributed by the cross section factors for the *p-p*, ^{3}He-^{4}He, and *p*-^{7}Be reactions. The reaction that produces ^{8}B depends upon a number of imperfectly known parameters and, since the production reaction is rare (see Table I), there is no independent constraint on the neutrino flux from the optically observed characteristics of the sun. For the neutrino fluxes from ^{13}N and ^{15}O decays, the largest contribution to the uncertainties is from the cross section factor for the *p*-^{14}N reaction.

TABLE XV. Total uncertainties in predicted neutrino fluxes from nuclear reaction rates, the solar constant, heavy element abundances, and the stellar density.

Neutrino source	Fractional uncertainty (3σ errors)
p-p	0.02
^{7}Be	0.29
^{8}B	0.52
^{13}N	0.5
^{15}O	0.55

The neutrinos from the proton-proton (and *pep*) reactions have the smallest calculated fractional uncertainty, 2%. This uncertainty is so small because the flux of *p-p* neutrinos is determined to a large extent by the measured solar constant and the fact that the ^{3}He-^{3}He reaction occurs much more frequently in the solar interior than the ^{3}He-^{4}He reaction.

General discussions of the experimental and theoretical possibilities for the detectors considered below are given in the *Proceedings of the Brookhaven Informal Conference on the Status and Future of Solar Neutrino Research* (BNL 50879), in Bahcall (1978, 1979), and in Cleveland, Davis, and Rowley (1980).

B. ^{7}Li

The first row of Table XVI gives the calculated uncertainties in the predicted rate for solar neutrino capture by ^{7}Li from the specified uncertainties in the rate of the proton-proton reaction, the ^{3}He-^{3}He reaction, the ^{3}He - ^{4}He reaction, the *p*-^{7}Be reaction, the heavy element abundance, and the solar opacity. Comparable uncertainties, all of order 4–6 SNU's, result from our imperfect knowledge of S_{11}, S_{34}, S_{17}, S_{114}, and Z; the other estimated uncertainties are relatively unimportant. The total estimated uncertainty is $\pm$ 14 SNU.

The predicted capture rate for solar neutrinos incident on a ^{7}Li target is

$$\sum_i \phi_i\sigma_i = 46.3\,\text{SNU}\,(1 \pm 0.30), \quad (25)$$

where 46.3 SNU is the value obtained with the neutrino fluxes calculated with the aid of the standard solar model and the effective 3σ error is $\pm$ 14.1 SNU. If the Munster value for S_{34} (Krawinkel *et al.* 1982) is used instead of the Caltech value (see discussion in Sec. II.A.5), then the rate predicted by the standard model is 37.2 SNU (1 ± 0.28).

The neutrino absorption cross sections used in the present calculation are given in Table XVII. The cross sections tabulated here differ somewhat from those given by Bahcall (1978), since the experimental *ft* value for the ^{7}Be decay to the $1/2^-$ excited state of ^{7}Li was changed

TABLE XVI. Uncertainties in predicted capture rates due to different parameters.

Uncertainty from parameter Detector indicated	$\delta(p\text{-}p)$ (SNU)	$\delta(^3\text{He}\text{-}^3\text{He})$ (SNU)	$\delta(^3\text{He}\text{-}^4\text{He})$ (SNU)	$\delta(p\text{-}^7\text{Be})$ (SNU)	δZ (SNU)	δOpacity (SNU)	δTotal (SNU)
^{7}Li	7.1	1.5	5.6	7.1	6.3	1.9	14
^{37}Cl	1.4	0.4	1.65	2.1	1.0	0.5	3.3[a]
^{71}Ga	3.5	1.6	6.3	0.6	3.2	1.3	$+12.5^{b}$ -8.7
^{81}Br	1.9	0.8	3.1	0.8	1.6	0.7	4.3[c]

[a] Includes 10% uncertainty in absorption cross sections for ^{8}B neutrinos (see Bahcall, 1978).
[b] Includes maximum likely contribution of 9 SNU from neutrino absorption to excited states (see Bahcall, 1978 and the text of this paper).
[c] Does not include uncertainty due to neutrino cross sections, which are taken from Bahcall (1981b).

incorrectly in the 1978 paper by multiplication with a statistical weight factor of one-half. The appropriate weighting factor was used earlier by Bahcall (1964, 1969) and by Domogatsky (1969). The capture rate given in Eq. (25) is 11% higher than would have been obtained with the incorrect cross sections.

Neutrinos from ^{8}B decay make the largest single contribution, 45%, to the counting rate expected on the basis of the standard solar model. Of the 30% overall uncertainty shown in Eq. (25), the greatest part, about 20%, is also from the flux of ^{8}B neutrinos; the quantities considered in Sec. II result in a total uncertainty due to neutrinos from ^{8}B decay of 10.3 SNU. However, the results of the ^{37}Cl experiment (Davis, 1978) suggest that the calculated flux of neutrinos from ^{8}B decay is overestimated by a factor of almost four (see Sec. V.C below).

The possibility of using a ^{7}Li detector for observing solar neutrinos has been discussed by, among others, Bahcall (1964b; 1969b), Kuzmin and Zatsepin (1966), Pomanski (1966), Davis (1969), and Rowley (1974; 1978).

C. ^{37}Cl

The uncertainties in the predicted capture rate for a ^{37}Cl detector are shown in the second row of Table XVI. The predicted capture rate is

$$\sum_i \phi_i \sigma_i = 7.6\,\text{SNU}\,(1 \pm 0.43). \tag{26}$$

TABLE XVII. Neutrino absorption cross sections for ^{7}Li.

Neutrino source	Cross section 10^{-46} cm^2
p-p	0
pep	646
^{7}Be	9.5
^{8}B	3.7×10^4
^{13}N	41.7
^{15}O	242

The estimated uncertainty in the flux of neutrinos from ^{8}B decay dominates the error indicated in Eq. (26). The uncertainty associated with the flux of neutrinos from ^{8}B decay accounts for 3.1 SNU out of a total of 3.3 SNU, about 94% of the total estimated uncertainty in the predicted rate.

The dependence of the predicted capture rate on individual parameters is given rather accurately by Eq. (8) of Bahcall, Bahcall, and Ulrich (1969), as may be shown by comparison of the values obtained with the formula derived in 1969 and the most recent values computed with the aid of the detailed results given in Tables VIII and XI–XIV.

The quantities that cause the largest uncertainties in the predicted capture rate are: S_{17} (2.1 SNU), S_{34} (1.7 SNU), S_{11} (1.4 SNU), and Z (1.0 SNU).

The ^{37}Cl experiment is primarily sensitive to neutrinos from ^{8}B decay. Approximately 80% of the predicted total capture rate is from these rare relatively high-energy neutrinos. The experimental results of Davis (1978) can be used to set an upper limit on the flux of neutrinos from ^{8}B decay: $\phi(^8\text{B}) \leq 2\times10^6$ cm^{-2}sec^{-1}. This upper limit is almost a factor of 4 less than the flux predicted by the standard model.

The capture rate given in Eq. (26) was computed using the value, and the estimated uncertainty, for the ^{3}He-^{4}He cross-section factor given in Eq. (8), which is consistent with the recent Caltech measurements (see Osborne *et al.* 1981). If we use instead the Munster value (see Krawinkel *et al.* 1982 and Sec. II.A.5 of this paper) with the large error quoted in Eq. (8) [i.e., $S_{34}(0) = 0.30 \pm 0.15$ keV b], we find (again quoting effective 3σ errors):

$$\sum_i \phi_i \sigma_i = 4.95\,\text{SNU}\,(1 \pm 0.42). \tag{27}$$

The estimated uncertainty in the flux of neutrinos from the decay of ^{8}B also dominates the error estimate in Eq. (27), accounting for 1.9 SNU out of a total of 2.1 SNU.

The ^{37}Cl experiment and its results have been described by Davis in a number of publications including Davis (1964; 1969; 1978), Davis and Harmer (1968),

Davis *et al.*. (1972), and Cleveland, Davis, and Rowley (1980). Theoretical discussions of this experiment are given in the references cited in the caption to Fig. 4 and in the many references contained therein.

D. ^{71}Ga

The uncertainties in the predicted capture rate for ^{71}Ga are given in the third row of Table XVI. We find

$$\sum_i \phi_i \sigma_i = 106.4\,\text{SNU}\,(1^{+0.12}_{-0.08}). \tag{28}$$

The predicted capture rate for ^{69}Ga is $\leq$ 0.1 SNU.

In calculating the rate given in Eq. (28), we have made use of the relatively recently measured lifetime for ^{71}Ge of 11.41 $\pm$ 0.06 d (Hampel, 1981b). Bahcall (1978) used a lifetime of 11.81 d to calculate the neutrino absorption cross sections for ^{71}Ga. Hence we have multiplied all of his cross sections for ^{71}Ga by a factor of 1.035.

The largest single uncertainty included in the error estimate of + 12.5 SNU shown in Table XVI is from possible transitions to excited states in ^{71}Ge. The estimates of total uncertainty in Table XVI and in Eq. (28) are not symmetric because transitions to excited states of ^{71}Ge can only increase the capture rate relative to what is calculated considering only transitions to ground states. The relevant excited states are: $5/2^-$ (at 0.175 MeV excitation), $3/2^-$ (at 0.50 MeV), and $3/2^-$ (at 0.71 MeV). We have followed the prescription of Bahcall (1978) in estimating the maximum likely contribution of transitions to these states. The correction factors Q_0 given in Table VIII of Bahcall (1978) were used to obtain a maximum possible increase in the cross section above the rate that is calculated by considering only ground state transitions. We find in this way a maximum contribution from transitions to excited states of ^{71}Ge of 9 SNU.

The strengths of the transitions to the three excited states of ^{71}Ge discussed above could be estimated by measuring the forward differential scattering cross section for the reaction ^{71}Ga$(p,n)^{71}$Ge at moderate energies ($>$ 100 MeV). Determination of the cross section to the ground state of ^{71}Ge and to the three relevant excited states should permit the independent estimation of normalized absolute values for the β-decay matrix elements. The (p,n) cross sections should yield reasonably accurate values for the relevant matrix elements (see Goodman *et al.* 1980). The method could be tested further by comparing the (p,n) cross sections for nuclei in the same mass range with related transitions (see Bahcall, 1978, for a list of the relevant target nuclei) with the known β-decay rates of the nuclei.

The proposed calibration of the ^{71}Ga detector with the aid of a ^{51}Cr source could also be useful in determining, or setting a limit on, the contributions from excited states. The maximum correction factors Q_0 used above correspond (cf. Bahcall, 1978) to an increase of the average cross section for neutrinos from ^{51}Cr by 15%, from 51.9×10^{-46} cm^2 to 59.5×10^{-46} cm^2.

The sources of uncertainty discussed in Sec. II lead to an uncertainty of 8.7 SNU in the predicted capture rate. The largest contributor to this uncertainty is the cross-section factor for the ^{3}He$(\alpha,\gamma)^7$Be reaction, which causes a 6 SNU uncertainty.

About 90% of the 8.7 SNU error estimated apart from the neutrino cross sections is caused by uncertainties in the predicted rate of the flux of ^{7}Be neutrinos. Unlike the ^{7}Li and ^{37}Cl experiments, the flux of neutrinos from the decay of ^{8}B contributes only a small inaccuracy ($<$1 SNU) to this error. The standard model gives a predicted rate due to neutrinos from ^{8}B decay of only 1.7 SNU (less than 2% of the total expected rate for this detector).

The flux of neutrinos from the basic proton-proton reaction contributes 67 SNU out of the predicted total of 106.4 SNU and might have been expected to affect significantly the estimated uncertainty in the total predicted capture rate. However, the calculated flux of neutrinos from this reaction is constrained by the requirement that the solar constant computed from the standard solar model be equal to the observed solar constant, which is known very accurately (see Sec. II.B). Since the flux of neutrinos from the proton-proton reaction is determined essentially by the observed solar photon luminosity (see Tables VIII, and XI–XIV), we find that *p-p* neutrinos contribute most (63%) of the expected counting rate in a gallium experiment, but very little ($\sim$2%) of the total estimated uncertainty.

If we use the Munster value for the cross section factor for the ^{3}He-^{4}He reaction (see Krawinkel *et al.* 1982, and Sec. II.A.5 of this paper), we obtain

$$\sum_i \phi_i \sigma_i = 96.7\,\text{SNU}\,(1^{+0.12}_{-0.08}). \tag{29}$$

Most of the difference between the rates given in Eqs. (28) and (29) is from neutrinos produced by electron capture on ^{7}Be.

The ^{71}Ga experiment was suggested by Kuzmin (1966). Various aspects of this experiment have been discussed by, among others, Pomanski (1965), Kuzmin and Zatsepin (1966), Dostrovsky (1978), Bahcall *et al.* (1978), Bahcall (1978), Cleveland, Davis, and Rowley (1980), and Hampel (1981a).

E. ^{81}Br

The known uncertainties in the predicted capture rate for a ^{81}Br target are given in the last row of Table XVI. The total estimated uncertainty, not including uncertainties in neutrino absorption cross sections, is 4.3 SNU, which is composed of comparable contributions from the rate of the *p-p* reaction, the rate of the ^{3}He-^{4}He reaction, and the primordial solar composition.

The predicted capture rate for a ^{81}Br detector is

$$\sum \phi_i \sigma_i = 16.6\,\text{SNU}\,(1 \pm 0.26), \tag{30}$$

where we have used the neutrino absorption cross sections given for ^{81}Br (and ^{79}Br) by Bahcall (1981b), which take account of the measurement of the metastable life-

time by Bennett *et al.* (1980; see also Haxton, 1981). The uncertainties in the neutrino absorption cross sections are difficult to evaluate with the available experimental data, but may be determinable by using a ^{51}Cr source (Bahcall, 1982) or by measuring (p,n) forward scattering cross sections at moderately high energies (cf. Goodman *et al.*, 1980). The largest fraction of the predicted rate, 10.6 SNU or 64%, is expected to arise from the ^{7}Be electron capture reaction.

If the Munster value for S_{34} (Krawinkel *et al.*, 1982) is used instead of the Caltech value (see discussion in Sec. II.A.5), then the rate predicted by the standard model is 11.6 SNU (1 ± 0.25).

For ^{79}Br, there is also a small capture rate of neutrinos from ^{8}B decay (Bahcall, 1981b). This rate is

$$\phi(^{8}\mathrm{B})\,\sigma(^{79}\mathrm{Br}) = 1.1\,\mathrm{SNU}\,(1 \pm 0.5). \tag{31}$$

If the Munster value for S_{34} is used instead of the Caltech value , then the right hand side of Eq. (31) must be multiplied by 0.63.

In addition to the references cited above, the ^{81}Br experiment has been discussed by, among others, Scott (1976, 1978), Hampel (1976), Rowley *et al.* (1980), and Hurst *et al.* (1980).

F. ^{115}In

The proposed experiment with ^{115}In (Raghavan 1976, 1978, 1981) involves measuring the energy of each electron produced by neutrino capture. The determination of the energy spectrum of the electrons, which reflects the energy spectrum of the neutrinos, would in principle make possible a separation of the different neutrino contributors to the total counting rate. Neutrinos from the proton-proton reaction contribute 81% of the predicted total capture rate and neutrinos from electron capture by ^{7}Be contribute 19%. The astrophysical uncertainties in the production rate from these two sources should be considered independently, since the electron spectra resulting from these reactions are to be measured separately.

We find, not including uncertainties in the neutrino absorption cross sections,

$$\phi(p\text{-}p)\,\sigma(^{115}\mathrm{In}) = 532\,\mathrm{SNU}\,(1 \pm 0.02), \tag{32}$$

and

$$\phi(^{7}\mathrm{Be})\,\sigma(^{115}\mathrm{In}) = 125\,\mathrm{SNU}\,(1 \pm 0.29). \tag{33}$$

If the Munster value for S_{34} is used instead of the Caltech value, then the right-hand side of Eq. (32) must be increased by 3% and the right-hand side of Eq. (33) multiplied by 0.61 (see Table VIII).

The additional uncertainties from the neutrino absorption cross sections are difficult to estimate reliably (see Bahcall, 1978). However, improved estimates of the neutrino cross sections could be obtained with the aid of measurements of (p,n) cross sections in the forward direction (see Goodman *et al.*, 1980) on ^{115}In leading to excited states of ^{115}Sn at excitation energies of 0.61 MeV and 1.25 MeV. (For *pep*, ^{8}B, ^{13}N, and ^{15}O neutrinos, the excited states at 1.62 MeV and 1.84 MeV could also be important.) The capture rates given in Eqs. (32) and (33) include transitions to only the $7/2^{+}$ state at 0.61 MeV.

G. $\nu_e - e$ scattering, ν_e absorption on ^{2}H, ^{97}Mo, and ^{98}Mo

The experiments that have been proposed to use either electron-neutrino scattering or neutrino absorption by deuterium to detect solar neutrinos are sensitive only to neutrinos from ^{8}B decay because the systems were designed to detect electrons that are scattered or produced above a threshold energy (usually chosen to be somewhere between 6 and 10 MeV) in order to limit the background. The predicted event rate depends sensitively on the threshold energy for electron detection. Hence we only quote for these experiments a fractional uncertainty in the predicted rate, $\delta R/R$, where (see Table XV):

$$\delta R(^{8}\mathrm{B})/R(^{8}\mathrm{B}) = \pm 0.52. \tag{34}$$

Either an electron-neutrino scattering experiment or a deuterium neutrino absorption experiment could give information about solar neutrinos from ^{8}B decay that is inaccessible from the ^{37}Cl or ^{71}Ga experiments. The ^{37}Cl experiment can be used to set an upper limit of 2×10^{6} solar neutrinos $\mathrm{cm}^{-2}\,\mathrm{sec}^{-1}$ from ^{8}B decay, but one cannot say how much of the observed counting rate is caused by neutrinos from ^{8}B decay. The ^{71}Ga experiment is insensitive to the flux of neutrinos from ^{8}B decay (see Table XVIII). A measurement, or an upper limit, on the flux of neutrinos from ^{8}B decay below 2×10^{6} $\mathrm{cm}^{-2}\,\mathrm{sec}^{-1}$ would provide independent and astrophysically important information (see Bahcall, 1978) on the rate at which the rare p-^{7}Be reaction occurs in the solar interior.

The absorption by ^{98}Mo (and ^{97}Mo) of solar neutrinos would produce trace amounts of Tc in deeply buried molybdenum ores and would yield information on the average neutrino flux from the decay of ^{8}B over the past several million years (see Cowan and Haxton, 1982). The results obtained from a Mo-Tc solar neutrino experiment would be complementary to, and independent of, results derived from measurements of the contemporary flux of neutrinos from ^{8}B decay. One cannot calculate accurately, with the available experimental information, the neutrino absorption cross sections to the various excited states of importance (cf. Cowan and Haxton, 1982). Hence we can only quote again the fractional uncertainty in the predicted rate, given in Eq. (34), that is independent of the (larger in this case) uncertainties from the neutrino absorption cross sections.

Some information about the flux of ^{7}Be neutrinos may be obtained by studying the production of ^{97}Tc in deeply buried molybdenum ores. The neutrino absorption cross sections for this process are also uncertain so we can only give the fractional uncertainty (see Table XV) in the flux of neutrinos from electron capture on ^{7}Be:

TABLE XVIII. The expected capture rates for the standard solar model. All capture rates are given in units of 1 SNU.

Source target	*p-p*	*pep*	^{7}Be	^{8}B	^{13}N	^{15}O	$\sum(\varphi\vartheta)$ Total
^{2}H[a]	0	0.0	0	6.7	0	0.0	6.7
^{7}Li[b]	0	9.7	4.1	20.7	2.1	9.7	46.3
^{37}Cl[a]	0	0.23	1.02	6.05	0.08	0.26	7.6
^{71}Ga[a]	67.2	2.4	28.5	1.7	2.7	3.8	106
^{79}Br[c]	0	0	0	1.1	0	0.0	1.1
^{81}Br[c]	0	1.2	10.6	2.2	1.0	1.6	16.6
^{115}In[a]	532	9.6	125	5.0	12.5	16	700

[a] Neutrino absorption cross sections from Bahcall (1978, 1979).
[b] Neutrino absorption cross sections from Table XVII.
[c] Neutrino absorption cross sections from Bahcall (1981b); see also Haxton (1982) and Bennett *et al.* (1981).

$$\delta R(^{7}\mathrm{Be})/R(^{7}\mathrm{Be}) = \pm 0.29. \tag{35}$$

One might hope that the *ratio* of neutrinos from ^{8}B decay to neutrinos from electron capture on ^{7}Be would be much better determined than either of the fluxes independently. Unfortunately, this is not the case since the main contributor to the uncertainty in the ratio, F, of the fluxes is the cross section factor for the reaction $p + {}^{7}$Be, which affects only $\phi(^{8}\mathrm{B})$ and not $\phi(^{7}\mathrm{Be})$. We find

$$\frac{\delta F}{F} = \pm 0.39, \tag{36}$$

where $F \equiv \phi(^{8}\mathrm{B})/\phi(^{7}\mathrm{Be})$.

Recent discussions of electron-neutrino scattering experiments have been given by Chen (1978) and Lande (1978). The use of deuterium as a detector of solar neutrinos has been discussed by Fainberg (1978). Cowan and Haxton (1982) have proposed using Tc isotopes produced by solar neutrino absorption in molybdenum ores to study the fluxes of neutrinos from ^{8}B decay and from electron capture by ^{7}Be.

VI. DISCUSSION AND CONCLUSIONS

We have determined limits within which the neutrino capture rates lie—provided that the flux of electron neutrinos from the sun is not diminished in transit and provided that there has not been a serious error in a measurement of an important experimental quantity nor a mistake in a theoretical calculation. We have also provided best estimates for a number of solar characteristics of general interest.

We summarize here the most important results and conclusions.

(1) Best estimates and effective 3σ uncertainties are given in Sec. II for all of the input parameters that affect in a significant way the prediction of solar neutrino capture rates. Opacities used in the present and previous calculations are compared in Tables V and VI.

The quantities that cause the largest recognized uncertainties are: the neutron lifetime, the low-energy nuclear cross sections for the ^{3}He$-^{4}$He, ^{1}H + ^{7}Be, and ^{1}H + ^{14}N reactions, the photospheric (or primordial) oxygen abundance, the solar radiative opacity, and, for some targets, neutrino absorption matrix elements to specified excited states. The Caltech and Munster experiments to determine the low-energy cross-section factor for the ^{3}He$-^{4}$He reaction are inconsistent with each other. For definiteness, we have adopted the Caltech value for our standard calculations, but we quote also the results obtained using the Munster value whenever the difference is important.

(2) The characteristics of a standard solar model are described in Sec. III. These include calculated results for the detailed run of the physical variables (Table VII), the solar neutrino fluxes (Table VIII and Fig. 2), and the luminosity history of the sun (Table IX). The calculational procedures are also discussed in this section and in the appendices.

(3) The primordial helium abundance implied by the standard solar model is $Y = 0.25 \pm 0.01$ (see Table X and Sec. III.C). This value is in good agreement with the primordial helium abundance inferred from the standard Big Bang cosmology (see Peebles, 1971). The assumed primordial oxygen abundance gives rise to a neutrino flux from the decay of ^{17}F that is comparable in numbers [see Eq. (18)] to the flux of neutrinos from the decay of ^{8}B. However, the lower-energy neutrinos from ^{17}F decay (with $E_{\mathrm{MAX}} = 1.7$ MeV) would not be detectable in any of the proposed solar neutrino experiments.

(4) Different regions of the sun make the dominant contribution to the following three observational quantities: (1) the 136 μHz splitting of the p-mode oscillations; (2) the solar luminosity (and the flux of p-p neutrinos); and (3) the flux of neutrinos from ^{8}B decay. This situation is illustrated in Fig. 3 (from Bahcall, 1981a) and Sec. III.C. We conclude that these three quantities are complementary in what they can reveal about the solar interior. In the future, standard solar models must, in order to be considered correct, be in agreement with all of the following: measurements of the solar luminosity, radius, neutrino capture rates, and

normal modes of oscillation. The interrelationship between the solar neutrino problem and the spectrum of p-mode oscillations is illustrated by the discussion of low-Z models given by Christensen-Dalsgaard, Gough, and Morgan (1979).

(5) Partial derivatives of each of the neutrino fluxes with respect to the important input parameters are given in Tables XI, XIII, and XIV and in Sec. IV. These partial derivatives were calculated with all but one (the quantity of interest) of the input parameters held fixed at its best-estimate value. We show by specific examples (see Tables VIII and XII) that the effects on the neutrino fluxes of even very large changes in the nuclear parameters can be calculated with acceptable accuracy using the tabulated partial derivatives.

Table XV lists the computed overall (effective 3σ) uncertainties in the individual neutrino fluxes that result from uncertainties in nuclear reaction rates, the solar constant, assumed primordial heavy element abundances, and solar opacity. The neutrinos from the proton-proton (and *pep*) reactions have the smallest calculated fractional uncertainty, 2%. The fractional uncertainty is 52% for the important flux of neutrinos from the decay of ^{8}B.

(6) The predicted capture rate for the ^{37}Cl solar neutrino experiment is [see Eq. (27)]: 7.6 ± 3.3 SNU (effective 3σ errors). The measured production rate is (Cleveland, Davis, and Rowley, 1981) 2.1 ± 0.3 SNU (1σ error).

The largest recognized uncertainties (see Sec. V.C) in the predicted capture rate are produced by uncertainties in the correct values for the primordial heavy element abundance, and in the nuclear cross sections for the ^{1}H$-^1$H, the ^{3}He$-^4$He, and the ^{7}Be$-^1$H reactions. The details are given in Sec. V.C.

There is a different way of estimating the overall uncertainty caused by the many parameters that must be used in a calculation of the predicted solar neutrino capture rate. We show in Fig. 4 all of the values for the predicted capture rate that have been published in this series of papers since the first discussion in 1964. For all cases in which estimates of the theoretical uncertainty were given, the originally published error bars are shown also in Fig. 4. After an initial period in which large uncertainties in the predicted rate were reduced (primarily by a much improved measurement of the rate of the ^{3}He$-^3$He reaction, see Tombrello, 1967), the value of 7.5 ± 3 SNU given by Bahcall and Shaviv (1968) has described the range of predicted rates derived with the aid of the numerous input parameters that have been continually revised because of improved measurements and/or theoretical calculations.

All of our standard calculations have been performed using the Caltech value for S_{34} (see Sec. II.A.5). If we use instead the Munster value for S_{34} (see Krawinkel, 1982, and Sec. II.A.5 of this paper), we find 4.95 ± 2.1 SNU (again effective 3σ errors). These results are discussed in more detail in Sec. V.C.

(7) Filippone and Schramm (1982) have estimated 1σ error limits for the ^{37}Cl experiment that are comparable to our calculated 3σ error limits. This difference is

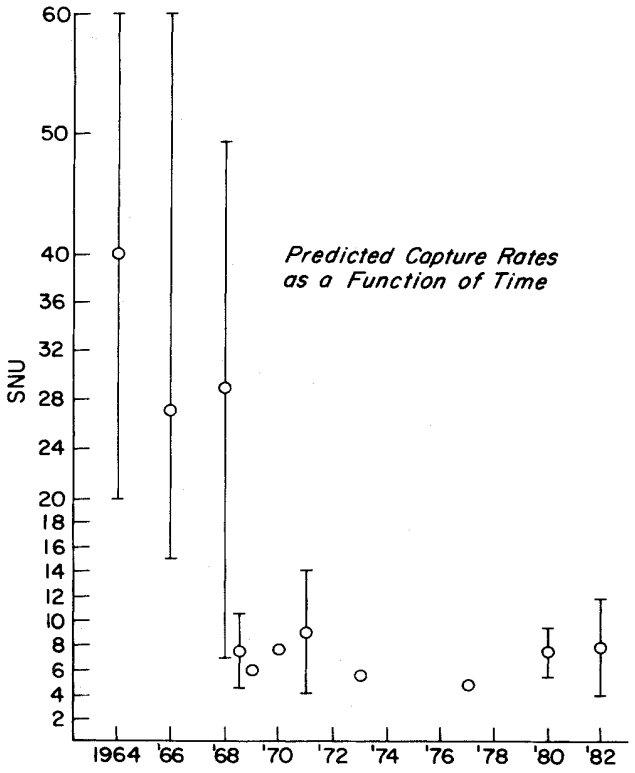

FIG. 4. Published values of the predicted neutrino capture rates from 1964 to 1980. The values and their error bars are from Bahcall (1964a), Bahcall (1966b), Bahcall and Shaviv (1968), Bahcall, Bahcall, Fowler, and Shaviv (1968), Bahcall, Bahcall, and Shaviv (1968), Bahcall (1969a), Bahcall and Ulrich (1970), Bahcall and Ulrich (1971), Bahcall, Huebner, Magee, Merts, and Ulrich (1973), Bahcall (1977), Bahcall, Huebner, Lubow, Magee, Merts, Parker, Rozsnyai, Ulrich, Argo (1980), and the present paper (1982). Similar results have been obtained by many other authors.

caused by their suprisingly large choices for the sizes of the errors. Filippone *et al.* (1982) assumed for the ^{3}He$(\alpha,\gamma)^4$He reaction that $S_{34}(0) = 0.52^{+0.15}_{-0.23}$ keV b, 1σ errors. Their average assumed 1σ error, 0.19 keV b, is more than six times the estimated error of either the Caltech or the Munster groups (see Sec. II.A.5) and, if interpreted naively at the 3σ level of uncertainty, suggests the possibility of a negative cross section. Filippone and Schramm (1982) have also reinterpreted in effect our 3σ error limits on the opacity that are illustrated in Table XIV as 1σ errors. However, more than half of the radiative opacity in the central regions of the sun is produced by photon scattering on free electrons and by inverse bremsstrahlung in the presence of completely ionized hydrogen and helium (see the last column of Table V and the discussion in Sec. II.D), processes that can be calculated with elementary quantum mechanics to an accuracy of better than 10%. Thus 1σ errors of 15%, or 3σ errors of 45%, are much larger than would be estimated for the Rosseland opacity in the central regions

of the sun using our current understanding of atomic physics or, in particular, by the LASL opacity group.

(8) The predicted capture rate for the ^{71}Ga experiment is [see Eq. (28)] $106(1^{+0.12}_{-0.08})$ SNU (effective 3σ errors). The relatively small overall uncertainty quoted for this detector is a direct result of the fact ^{71}Ga is primarily sensitive to neutrinos from the basic proton-proton reaction, the rate of which is determined largely by the observed solar luminosity. Possible transitions to excited states in ^{71}Ge, cause a large part of the uncertainty in this predicted rate, namely 9 SNU. This uncertainty could be reduced by measuring the forward differential scattering cross section of the reaction ^{71}Ga$(p,n)^{71}$Ge and by a source experiment using ^{51}Cr. Most of the other uncertainty quoted above in the predicted capture rate comes from an uncertainty in the flux of neutrinos from electron capture by ^{7}Be.

The Munster value for S_{34} leads to a predicted capture rate of 97 SNU [see Eq. (29)].

(9) The expected capture rates from each neutrino source are given in Table XVIII for all of the targets considered here with the exception of electron-neutrino scattering targets and molybdenum isotopes, both of which are discussed in Sec. V.G. The ^{2}H, ^{37}Cl, molybdenum, and electron scattering targets are primarily sensitive to neutrinos from ^{8}B decay, the ^{71}Ga and ^{115}In detectors to neutrinos from the *p-p* reaction, the ^{81}Br target to neutrinos from electron capture on ^{7}Be, and ^{7}Li to several neutrino branches (most importantly, neutrinos from ^{8}B and ^{15}O decay and from the *pep* reaction).

(10) The Caltech and Munster measured values for the cross-section factor for the reaction ^{3}He$(\alpha,\gamma)^{4}$He are inconsistent with each other (see discussion in Sec. II.A). We have calculated a series of standard solar models using progressively smaller values for the cross-section factor $S_{34}(0)$, while holding all of the other input parameters constant at their standard values. We find that in order to obtain agreement with the observations of Davis (1978) (see also Cleveland, Davis, and Rowley, 1981) for the ^{37}Cl experiment (i.e., a capture rate of 2 SNU), the cross-section factor $S_{34}(0)$ must be reduced to 0.09 keV b, which is, using the errors quoted by the experimental groups, about 15σ less than the Caltech value or 7σ less than the Munster value.

ACKNOWLEDGMENTS

We are grateful to D.L. Lambert for permission to summarize his important analysis of the uncertainties in the determination of the photospheric oxygen abundance and to many other colleagues for discussing with us in detail their published measurements or calculations. One of us (J.N.B.) wishes to express his appreciation to G. V. Domogatsky for his remarks about the ^{7}Li cross sections, to R. W. Kavanagh for providing us with the original data for his important experiment on proton capture by ^{7}Be, and to W. A. Fowler and M. Schwarzschild for their valuable advice and encouragement at the time, four years ago, when this project was begun and for helpful suggestions on many subsequent occasions. J.N.B. especially wishes to thank R. Soneira for his generous and expert help in carrying out the many calculations of solar models that were made at the Princeton University computing center. His gracious assistance made possible the extensive parameter variations that are described in this paper. This work has been supported by NSF Grant No. PHY79-19884 at the Institute for Advanced Study, NSF Grant No. AST80-19745 at the University of California, Los Angeles, under the auspices of the United States Department of Energy at Los Alamos Scientific Laboratory, and DOE Contract No. DE-ACO2-76 ERO3074 at Yale University.

APPENDIX A: TREATMENT OF THE "ATMOSPHERE ZONE"

The solar structure code truncates the solar model at a point above which about $10^{-3}M_{\odot}$ remains. At this point the temperature is about 3×10^{5} K and most of the complications relating to partial ionization of hydrogen and helium can be neglected. Numerical tests have shown that this "atmosphere zone" has only a very minor and indirect impact on the solar neutrino flux, so we have adopted a fairly crude treatment of this region. The last point below the surface generally falls in the convective envelope, so we can crudely describe the outer zone with a polytropic equation:

$$T = KP^{0.4}. \tag{A1}$$

The exponent 0.4 is valid for much of the atmosphere zone, and Eq. (A1) is adequate for our application. The polytropic constant is related to an entropylike variable by

$$S - S_0 = 2.5\log K, \tag{A2}$$

where the additive constant S_0 is dependent on the behavior of the gas near 0 K and on dimensional factors. For convenience we take $S_0 = 0$ for T and P measured in cgs units. An interpolation formula for S based on a grid of model envelopes for T_e and L near $(T_e)_{\odot}$ and $L_{\odot}$ is

$$S = S_e + 0.27t + 0.04t^2 + 0.095m + 0.06mt; \tag{A3}$$

where

$$m = -(M_{BOL} - 3.5)/2, \tag{A4}$$

$$t = (\log T_e - 3.65)/20, \tag{A5}$$

and

$$M_{BOL} = 4.78 - 2.5\log(L/L_{\odot}). \tag{A6}$$

Here S_e is an adjustable constant dependent on the value of l. Table XIX gives a comparison of the value of S calculated from Eq. (A3) to the values computed with the atmosphere code described by Ulrich and Rhodes (1977). The value of S_e used in this comparison was

TABLE XIX. Comparison of S_{model} to $S_{(A3)}$.

M_{BOL}		$\log T_e$ 3.65	3.70	3.75	3.80
3.5	S_{model}	1.765	2.078	2.492	2.855
	$S_{(A3)}$	1.770	2.080	2.470	2.940
4.0	S_{model}	1.643	1.889	2.221	2.675
	$S_{(A3)}$	1.675	1.925	2.255	2.665
4.5	S_{model}	1.595	1.725	2.001	2.476
	$S_{(A3)}$	1.580	1.770	2.040	2.390
5.0	S_{model}	1.458	1.596	1.813	2.251
	$S_{(A3)}$	1.485	1.615	1.825	2.115
5.5	S_{model}	1.309	1.462	1.627	
	$S_{(A3)}$	1.390	1.460	1.610	

1.77. Because the adopted standard value of $L_\odot$ has changed by a small amount, we have worked out the various numerical factors such as (A6) assuming a fixed value of $L_\odot$ which is 3.86×10^{33} ergs sec^{-1}. This luminosity and an adopted solar radius of 6.96×10^{10}cm leads to $(T_e)_\odot = 5783$ K.

The atmosphere zone is entered with specified values of M_{BOL} and log T_e. The outer radius is then calculated from

$$R = R_\odot \left[\frac{L}{L_\odot}\right]^{1/2} \left[\frac{(T_e)_\odot}{T_e}\right]^2. \tag{A7}$$

The values of S and K are found from Eqs. (A2)–(A6). The mass of the atmosphere zone is defined at the beginning of a model sequence and remains fixed. Let this mass be ΔM. Hydrostatic equilibrium gives

$$P = \frac{GM}{4\pi R^4}\,\Delta M \tag{A8}$$

provided that $\Delta M \ll M$ and the radius increment across the atmosphere Δr is much less than R. We assume that the mean molecular weight is constant through the bulk of the atmosphere zone. The density is then given by

$$\rho = \frac{\mu P^{0.6}}{RK} \tag{A9}$$

where R is the gas constant. The equation of hydrostatic equilibrium gives

$$\Delta r = \frac{2.5RK}{\mu(GM)^{0.6}} \left[\frac{R\Delta M}{4\pi}\right]^{0.4}. \tag{A10}$$

Equation (A10) is accurate to about ten percent for $\Delta M \sim 10^{-3} M_\odot$. The four variables at the inner edge of the atmosphere zone are given by Eqs. (A1), (A8), and

$$L_r = L_{\text{surface}}, \tag{A11}$$

$$r = R - \Delta r. \tag{A12}$$

APPENDIX B: TREATMENT OF THE NUCLEAR ABUNDANCES

The hydrogen burning reactions form two more or less independent sets: the *p-p* chain and the CNO cycle. Three classes of species appear in the abundance network which describes these reactions: (1) species which are either fuels or products and which have slowly varying abundances, (2) minor species whose abundances can be assumed to have steady-state values, and (3) species which are intermediate between class one and two. Class (2) species can generally be eliminated from the reaction network. Examples of such species are ^{2}H, ^{7}Li, ^{7}Be, and ^{13}N. Class (1) species can be treated with a variety of methods without causing numerical problems. Class (3) species cause some problems because they cannot be eliminated from the abundance network in that part of the stellar model where they behave like class (1) species. One solution is to devise several reaction networks dependent on the sets of species which are in steady state. Disadvantages of this approach are the increase in complexity of the code and the introduction of numerical discontinuities in changing from one network to another. Another solution, adopted here, is to include the class (2) species throughout the model and to use a single reaction network. In order to avoid numerical instabilities in those zones where the species lifetime is shorter than the time step, the abundance equations must be written in a backwards difference format.

For the case of ^{3}He, the most important class (2) species, the abundance equation is

$$A_3^{-1} \frac{dX_3}{dt} = R_{11}X_1^2 - R_{34}X_3X_4 - 2R_{33}X_3^2, \tag{B1}$$

where X_i is the mass fraction of species i. Also R_{ij} is related to λ_{ij} of Fowler, Caughlan, and Zimmerman (1967) by

$$R_{ij} = \left[\rho N_A \lambda_{ij} \,/\, (1+\delta_{ij}) A_i A_j\right] \tag{B2}$$

where N_A is Avogadro's number, δ_{ij} is the Kroneker del-

ta, and A_i is the atomic mass of species i. We designate with a superscript n the values of the abundances and rates at the previous time step. The backward difference form of Eq. (B1) is

$$\frac{X_3 - X_3^n}{A_3 \Delta t} = R_{11} X_1^2 - R_{34} X_3 X_4 - 2R_{33} X_3^2. \quad \text{(B3)}$$

Equations like (B3) can be written for each species. Because ^{3}He must be treated with a backwards difference equation, all other species must be treated this way as well. The forward difference form of (B3) would consist of adding superscript n's to all quantities on the right. A nonlinear set of equations for the abundances results from the complete set of conservation equations. This set could be solved by linearization and matrix inversion, but it is simple enough that an *ad hoc* scheme is more efficient. We guess a value for X_1 and X_3 by extrapolation, calculate X_4 from $1-X_1-X_3-X_{12}-X_{14}-X_{16}-X_{\text{heavy}}$, then calculate a new value for X_3 by solving the quadratic equation (B3).

The above scheme for following the abundances provides for a fully self-consistent treatment of the nuclear evolution throughout the solar model. However, it has a built-in characteristic which makes its implementation awkward in some respects. The rates in the nuclear network depend on the temperature and density. The state variables depend on the composition so that the network of abundances is coupled to the equations of stellar structure in a complicated way. If the dependence of the composition on temperature and density is neglected, it can cause convergence problems under some circumstances. We have broken the coupling of state variables and composition by recalculating the composition for each temperature and density. The solar model is constructed by a series of fourth-order Runge-Kutta integrations from the center outward and from the surface inward. At each point in the integrations the temperature and pressure are known from the differential equations. The density is found from the equation of state. At this point the composition is not known because it depends on the density. It has proven satisfactory to use the composition from the previous unperturbed integration. Numerical derivatives at the matching point are found from a series of perturbed trial integrations. Abundances from perturbed integrations should not be used to calculate the density. After the density is found then the abundances are determined and the nuclear energy generation is calculated. Thus the rate of nuclear energy generation is always correctly calculated, while a small error in the equation of state is tolerated during the convergence process. (No satisfactory analogous method of treating a convective core was found. Fortunately, the standard solar model does not have a convective core, and this difficulty did not need to be confronted.)

One conceivable way of avoiding the complications discussed above is to use reaction rates based on previous time steps. The nuclear energy generation rate must be calculated from abundances and rates that are self-consistent in order to ensure that the proper amount of energy is released through the conversion of hydrogen to helium. Alternatively, the composition parameters could be included in the variational scheme with the same standing as pressure and temperature. This latter alternative would probably not simplify the numerical algorithm, but is probably the only way to treat a convective zone.

Another problem with a backwards difference scheme results from changes in the reaction rates during the evolution. In general, steady-state species like ^{3}He should have an abundance given by $dX_3/dt = 0$. Since the values of R_{ij} and X_i change during the evolution, the steady-state value also changes. Near steady state the equation for the abundance X has the form

$$\frac{dX}{dt} = R(X_{SS} - X) \quad \text{(B4)}$$

where X_{SS} is the steady-state abundance. If the abundance at the beginning of the time step is X_0, then the backwards difference value of X is

$$X = X_{SS} + (X_0 - X_{SS})(1 + R\Delta t)^{-1}, \quad \text{(B5)}$$

whereas the solution to Eq. (B4) should be

$$X = X_{SS} + (X_0 - X_{SS}) e^{-R\Delta t}. \quad \text{(B6)}$$

For large values of $R\Delta T$ the difference between $(1+R\Delta t)^{-1}$ and $\exp(-R\Delta t)$ is substantial, and undesirable numerical disequilibrium can result. In order to reduce this problem we have subdivided each time step into a sequence of smaller subtime steps. The reaction rates at each substep are found by interpolation between the trial value at the advanced time and the converged value at the preceding time. The nuclear reaction network is then entered in the normal fashion and the abundance advanced through the sequence of substeps, for each point. If there are N substeps, this process represents $\exp(-R\Delta t)$ by $(1+R\Delta t/N)^{-N}$. For large N the representation becomes exact.

To study the size of the error for finite N define:

$$D = (1 + R\Delta t/N)^{-N} - e^{-R\Delta t}, \quad \text{(B7)}$$

so that the numerical representation of Eq. (B6) becomes

$$X = X_{33} + (X_0 - X_{33}) e^{-R\Delta t} + (X_0 - X_{33}) D, \quad \text{(B8)}$$

where the last term represents a numerical error introduced by the algorithm. For $N = 1$, D reaches a maximum of 0.204 at $R\Delta t = 2.5$ and decreases only as $(R\Delta t)^{-1}$ for larger $R\Delta t$. For $N = 3$, the maximum value of D is 0.081 at $R\Delta t = 2.2$, and D drops below 10^{-3} at a $R\Delta t = 27$. In practice, the behavior at large $R\Delta t$ is most important, and $N = 3$ has proven satisfactory.

REFERENCES

Avni, Y., 1978, Astron. Astrophys. **66**, 307.
Bahalla, C. P., 1966, Phys. Lett. **19**, 691.

Bahcall, J. N., 1962, Phys. Rev. **128**, 1297.
Bahcall, J. N., 1964a, Phys. Rev. Lett. **12**, 300.
Bahcall, J. N., 1964b, Phys. Lett. **13**, 332.
Bahcall, J. N., 1966a, Nucl. Phys. **75**, 10.
Bahcall, J. N., 1966b, Phys. Rev. Lett. **17**, 398.
Bahcall, J. N., 1969a, in *Proceedings of the International Conference on Neutrino Physics and Astrophysics* (F. I. Acad. Sci. USSR, Moscow), Vol. 2, p. 133.
Bahcall, J. N., 1969b, Phys. Rev. Lett. **23**, 251.
Bahcall, J. N., 1977, Astrophys. J. Lett. **216**, 115.
Bahcall, J. N., 1978, Rev. Mod. Phys. **50**, 881–904.
Bahcall, J. N., 1979, Space Sci. Rev. **24**, 227.
Bahcall, J. N., 1981a, in *Neutrino 81,* edited by R. J. Cence, E. Ma, and A. Roberts, (University of Hawaii High Energy Physics Group), Vol. 2, p. 253.
Bahcall, J. N., 1981b, Phys. Rev. C **24**, 2216.
Bahcall, J. N., N. A. Bahcall, and G. Shaviv, 1968, Phys. Rev. Lett., **20**, 1209.
Bahcall, J. N., N. A. Bahcall, and R. K. Ulrich, 1969, Astrophys. J. **156**, 559.
Bahcall, J. N., B. T. Cleveland, R. Davis, Jr., I. Dostrovsky, J. C. Evans, Jr., W. Frati, G. Friedlander, K. Lande, J. K. Rowley, W. Stoenner, and J. Weneser, 1978, Phys. Rev. Lett. **40**, 1351.
Bahcall, J. N., W. F. Huebner, N. H. Magee, A. L. Merts, and R. K. Ulrich, 1973, Astrophys. J. **184**, 1.
Bahcall, J. N., S. H. Lubow, W. F. Huebner, N. H. Magee, Jr., A. L. Merts, M. F. Argo, P. D. Parker, B. Rozsnyai, and R. K. Ulrich, 1980, Phys. Rev. Lett. **45**, 945.
Bahcall, J. N., and R. M. May, 1969, Astrophys. J. **155**, 501.
Bahcall, J. N., and C. P. Moeller, 1969, Astrophys. J. **155**, 511.
Bahcall, J. N., and R. L. Sears, 1972, Annu. Rev. Astron. Astrophys., **10**, 25.
Bahcall, J. N., and G. Shaviv, 1968, Astrophys. J., **153**, 113.
Bahcall, J. N., and R. K. Ulrich, 1970, Astrophys. J. **160**, L57.
Bahcall, J. N., and R. K. Ulrich, 1971, Astrophys. J. **170**, 593
Bargholtz, C., 1979, Astrophys. J. Lett. **233**, L161.
Barker, F. C., 1979, private communication.
Barker, F. C., 1980, Aust. J. Phys., **33**, 177.
Bennett, C. L., M. M. Lowry, R. A. Naumann, F. Loeser, and W. Moore, 1980, Phys. Rev. C **22**, 2245.
Bethe, H. A., 1939, Phys. Rev. **55**, 434.
Blin-Stoyle, R. J., and J. M. Freeman, 1970, Nucl. Phys. A **150**, 369.
Blin-Stoyle, R. J., and S. Papageorgiou, 1965, Nucl. Phys. **64**, 1.
Bondarenko, L. N., V. V. Kurguzov, Yu. A. Prokof'ev, E. V. Rogov, and P. E. Spivak, 1978, JETP Lett. **28**, 303.
Brown, L., E. Steiner, L. G. Arnold, and R. Seyler, 1973, Nucl. Phys. A **206**, 353.
Byrne, J., J. Morse, K. F. Smith, F. Shaikh, K. Green, and G. L. Greene, 1980, Phys. Lett. B **92**, 274.
Cameron, A. G. W., 1973, Space Sci. Rev., **15**, 121.
Cameron, A. G. W., 1982, in *Essays in Nuclear Astrophysics,* edited by C. A. Barnes, D. D. Clayton, and D. N. Schramm (Cambridge University Press, Cambridge, England), Chap. 3, pp. 23–43.
Carson, T. R., 1976 (private communication to W. Huebner).
Cash, W., 1976, Astron. Astrophys. **52**, 307.
Chen, H. H., 1978, in *Proceedings of Informal Conference on Status and Future of Solar Neutrino Research,* edited by G. Friedlander (Brookhaven National Laboratory Report BNL 50879), Vol. 2, p. 55.
Chen, C. H., 1980, Phys. Today, **33**(9), 24.
Christensen, C. J., A. J. Nielsen, A. Bahnsen, W. K. Brown, and B. M. Rustach, 1967, Phys. Lett. B **26**, 11.
Christensen, C. J., A. J. Nielsen, A. Bahnsen, W. K. Brown, and B. M. Rustach, 1972, Phys. Rev. D **5**, 1628.
Christensen-Dalsgaard, J., and D. O. Gough, 1980, Nature **288**, 544.
Christensen-Dalsgaard, J., D. O. Gough, and J. G. Morgan, 1979, Astron. Astrophys. **73**, 121.
Claverie, A., G. R. Issak, C. P. McLeod, H. B. Van der Raay, and T. Roca Cortes, 1979, Nature **282**, 591.
Clayton, D. D., 1968, *Principles of Stellar Evolution and Nucleosynthesis* (McGraw-Hill, New York), p. 612.
Cleveland, B. T., R. Davis, Jr., and J. K. Rowley, 1980, in *Proceedings of the Neutrino Miniconference,* University of Wisconsin Report No. 186 (University of Wisconsin, Madison), p. 38.
Cleveland, B. T., R. Davis, Jr., and J. K. Rowley, 1981, in *Weak Interactions as Probes of Unification,* edited by G. B. Collins, L. N. Chang, and J. R. Fience (AIP Conference Proceedings No. 72), p. 322
Cowan, G. A., and W. C. Haxton, 1982, Science **216**(4541), 51.
Dautry, F., M. Rho, and D. O. Riska, 1976, Nucl. Phys. A **264**, 507.
Davis, R., Jr., 1964, Phys. Rev. Lett. **12**, 303.
Davis, R., Jr., 1969, in *Proceedings of the International Conference on Neutrino Physics and Astrophysics* (F. I. Acad. Sci. USSR, Moscow), Vol. 2, p. 99.
Davis, R., Jr., 1978, in *Proceedings of Informal Conference on Status and Future of Solar Neutrino Research,* edited by G. Friedlander (Brookhaven National Laboratory Report No. BNL 50879), Vol.1, p. 1.
Davis, R., Jr., J. C. Evans, V. Radeka, and L. I. Rogers, 1972, in *Neutrino '72,* edited by A. Frenkel and G. Marx (OMDK - Technoinform, Budapest), Vol. 1, p. 5.
Davis, R., Jr., D. S. Harmer, and K. C. Hoffman, 1968, Phys. Rev. Lett. **20**, 1205.
Deubner, F. L., 1975, Astron. Astrophys. **44**, 371.
Deubner, F. L., R. K. Ulrich, and E. J. Rhodes, Jr., 1979, Astron. Astrophys. **72**, 177.
Diesendorf, M. O., 1970, Nature **227**, 266.
Dobrozemsky, R., E. Kerschbaum, G. Moraw, H. Paul, C. Stratowa, and P. Weinzierl, 1975, Phys. Rev. D **11**, 510.
Domogatsky, G. V., 1969, Lebedev Phys. Inst. Report No. 153.
Dostrovsky, I., 1978, in *Proceedings of Informal Conference on Status and Future of Solar Neutrino Research,* edited by G. Friedlander, (Brookhaven National Labortory Report BNL 50879), Vol.1, p. 231.
Dwarakanath, M. R., 1974, Phys. Rev. C **9**, 805.
Dwarakanath, M. R., and H. Winkler, 1971, Phys. Rev. C **4**, 1532.
Ebeling, W., W. D. Kraft, and D. Krenp, 1977, *Theory of Bound States and Ionization Equilibrium in Plasmas and Solids* (Akademie-Verlag, Berlin).
Ebeling, W., and R. Sändig, 1973, Ann. Phy. (Leipzig) **28**, 289.
Elwyn, A. J., R. E. Holland, C. N. Davids, and W. Ray, Jr., 1982 (unpublished).
Fainberg, A. M., 1978, in *Proceedings of Informal Conference on Status and Future of Solar Neutrino Research,* edited by G. Friedlander (Brookhaven National Laboratory Report BNL 50879), Vol. 2, p. 93.
Fetisov, V. N., and Yu. S. Kopysov 1972, Phys. Lett. B **40**,

602.
Filippone, B. W., A. J. Elwyn, W. Ray, Jr., and D. D. Koetke, 1982 (unpublished).
Fowler, W. A., 1972, Nature **238**, 24.
Fowler, W. A., G. R. Caughlan, and B. A. Zimmerman, 1967, Annu. Rev. Astron. Astrophys. **5**, 525.
Fowler, W. A., G. R. Caughlan, and B. A. Zimmerman, 1975, Annu. Rev. Astron. Astrophys. **13**, 69.
Gari, M., 1978, in *Proceedings of Informal Conference on Status and Future of Solar Neutrino Research,* edited by G. Friedlander (Brookhaven National Labortory Report BNL 50879), Vol. 1, p. 137
Gari, M., and A. Huffman, 1973, Phys. Rev. C **7**, 994.
Goodman, C. D., C. A. Goulding, M. B. Greenfield, J. Rapaport, D. E. Bainum, C. C. Foster, W. G. Love, and F. Petrovich, 1980, Phys. Rev. Lett. **44**, 1755.
Gough, D. O., 1978, "Pleins feux sur la physique solaire," in *Proceedings of the 2nd European Assembly in Solar Physics,* edited by J. Rösch (CNRS, Paris), p. 81—103.
Grec, G., E. Fossat, and M. Pomerantz, 1980, Nature **288**, 541.
Griffiths, G. M., M. Lal, and C. D. Scarfe, 1963, Can. J. Phys. **41**, 724.
Halbert, M. L., D. C. Hensley, and H. G. Bingham, 1973, Phys. Rev. C **8**, 1226.
Hampel, W., 1976, Annual Report, MPI Kernphysik, 158.
Hampel, W., 1981a, in *Neutrino 81,* edited by R. J. Cence, E. Ma, and A. Roberts, (University of Hawaii High Energy Physics Group), Vol. 1, p. 6.
Hampel, W., 1981b (private communication).
Hauge, O., and O. Engvold, 1977, Compilation of Solar Abundance Data, Report No. 49, Institute of Theoretical Astrophysics, Blinden-Oslo.
Haxton, W. C., 1981, Nucl. Phys. A **367**, 517.
Haxton, W., 1982, in preparation.
Hickey, J. R., L. L. Stowe, H. Jacobowitz, P. Pellegrino, R. H. Maschhoff, F. House, and T. H. Vonder Haar, 1980, Science **208**, 281.
Holweger, H., 1979, in *Les Elements et Leurs Isotopes dans L'Univers,* 22nd Liège International Astrophysics Symposium (University of Liège, Liège), p. 117.
Huebner, W. F., 1978, in *Proceedings of Informal Conference on Status and Future of Solar Neutrino Research,* edited by G. Friedlander (Brookhaven National Laboratory Report No. BNL 50879), Vol. 1, p. 107.
Huebner, W. F., 1982, "Atomic and Radiative Processes in the Solar Interior," in *Advocacy Document on the Physics of the Sun,* edited by P. Sturrock, to be published.
Huebner, W. F., A. L. Merts, N. H. Magee, Jr., and M. F. Argo, 1977, Astrophysical Opacity Library, Los Alamos Scientific Laboratory Report No. LA-6760-M.
Hurst, G. S., M. G. Payne, S. Kramer, and C. H. Chen, 1980, Phys. Today **33**(9), 24.
Iben, I., Jr., 1968, Phys. Rev. Lett. **21**, 1208.
Iben, I., K. Kalata, and J. Schwartz, 1967, Astrophys. J. **150**, 1001.
Iben, I., Jr., and J. Mahaffy, 1976, Astrophys. J. **209**, L39.
Issak, G. R., 1980, Nature **283**, 644.
Kalnin, A., and P. D. Parker, 1981, private communication.
Kavanagh, R. W., 1960, Nucl. Phys. **15**, 411.
Kavanagh, R. W., 1972, in *Cosmology, Fusion, and Other Matters,* edited by F. Reines (University of Colorado, Denver), p. 169.
Kavanagh, R. W., T. A. Tombrello, J. M. Mosher, and D. R. Goosman, 1969, Bull. Am. Phys. Soc. **14**, 1209.
Kim, B. T., T. Izumato, and K. Nagatani, 1981, Phys. Rev. C **23**, 33.
Krawinkel, H., H. W. Becker, L. Buchmann, G. Gorres, K. N. Kettner, W. E. Kieser, R. Santo, T. Schmalbrock, H. P. Trautvetter, A. Vlieks, C. Rolfs, J. W. Hammer, R. E. Azuma, and W. S. Rodney, 1982, Z. Phys. A, **304**, 307.
Krohn, V., and G. Ringo, 1975, Phys. Lett. B **55**, 175.
Kuzmin, V. A., 1966, Sov. Phys.—JETP **22**, 1051.
Kuzmin, V. A., and G. T. Zatsepin 1966, in Proceedings of the International Conference on Cosmic Rays, London, Vol. 2, p. 1023.
Lambert, D. L., 1978, Mon. Not. R. Astron. Soc. **182**, 249.
Lambert, D. L., 1981, private communication.
Lambert, D. L., and R. E. Luck, 1978, Mon. Not. R. Astron. Soc. **183**, 79.
Lambert, D. L., and B. Warner, 1968, Mon. Not. R. Astron. Soc. **140**, 197.
Lande, K., 1978, in *Proceedings of Informal Conference on Status and Future of Solar Neutrino Research,* edited by G. Friedlander (Brookhaven National Laboratory Report No. BNL 50879), Vol. 2, p. 79.
Larkin, A. I. 1960, Sov. Phys.—JETP **11**, 1363.
Leckrone, D. S., 1971, Astron. Astrophys. **11**, 387.
Leibacher, J., and R. F. Stein, 1971, Astrophys. Lett. **7**, 191.
Leighton, R. B., 1961, Nuovo Cimento Suppl. **22**,.
Leighton, R. B., R. W. Noyes, and G. W. Simon, 1962, Astrophys. J. **135**, 474.
Lerner, G. M., and J. B. Marion, 1969, Nucl. Instrum. Methods **69**, 115.
Liu, Q. K. K., H. Kanada, and Y. C. Tang, 1981, Phys. Rev. C **23**, 645.
Lubow, S. H., R. K. Ulrich, M. F. Argo, W. F. Huebner, N. H. Magee, and A. L. Merts, 1979, Bull. Am. Astron. Soc. **10**, 676.
Magee, N. H., Jr., A. L. Merts, and W. F. Huebner, 1975, Astrophys. J. **196**, 617.
McClenahan, C. R., and R. E. Segel, 1975, Phys. Rev. C **11**, 370.
Meyer, J. P., 1979, in *Les Elements et Leurs Isotopes dans L'Univers,* 22nd Liège International Astrophysics Symposium (University of Liège, Liège), p. 153.
Mingay, D. W., 1979, S. Afr. Tydskr. Fis. **2**, 107.
Nagatani, K., M. R. Dwarakanath, and D. Ashery, 1969, Nucl. Phys. A **128**, 325.
Osborne, J. L., C. A. Barnes, R. W. Kavanagh, R. M. Kremer, G. J. Mathews, J. L. Zyskind, P. D. Parker, and A. J. Howard 1981, Bull. Am. Phys. Soc. **26**, 565.
Pagel, B. E. J., 1973, Space Sci. Rev. **15**, 1.
Parker, P. D., 1966, Phys. Rev. **150**, 851.
Parker, P. D., 1968, Astrophys. J. **153**, L85.
Parker, P. D., 1978, in *Proceedings of Informal Conference on Status and Future of Solar Neutrino Research,* edited by G. Friedlander (Brookhaven National Laboratory Report No. BNL 50879), Vol.1, p. 77.
Parker, P. D., 1982, "Thermonuclear Reactions in the Solar Interior" in *Advocacy Document on the Physics of the Sun,* edited by P. Sturrock (to be published).
Parker, P. D., J. N. Bahcall, and W. A. Fowler, 1964, Astrophys. J. **139**, 602.
Parker, P. D., and R. W. Kavanagh, 1963, Phys. Rev. **131**, 2578.
Parker, P. D., D. J. Pisano, M. E. Cobern, and G. H. Marks, 1973, Nat. Phys. Sci. **241**, 106.

Peebles, P. J. E., 1971, *Physical Cosmology* (Princeton University, Princeton, N.J.).
Peimbert, M., and S. Torres-Peimbert, 1977, Mon. Not. R. Astron. Soc. **179**, 217.
Pomanski, A. A., 1965, "On the Possibility of Utilizing ^{71}Ga as a Detector of Solar Neutrinos" (Report, Lebedev Physical Institute).
Pomanski, A. A., 1966, "Practical Possibilities of Utilizing ^{71}Ga as a Detector of Solar Neutrinos" (Report, Lebedev Physical Institute).
Raghavan, R. S., 1976, Phys. Rev. Lett. **37**, 259.
Raghavan, R. S., 1978, in *Proceedings of Informal Conference on Status and Future of Solar Neutrino Research,* edited by G. Friedlander (Brookhaven National Laboratory Report No. BNL 50879), Vol. 2, p. 1.
Raghavan, R. S., 1981, in *Neutrino 81,* edited by R. J. Cence, E. Ma, and A. Roberts (University of Hawaii High Energy Physics Group), Vol. 1, p. 27.
Rhodes, E. J., Jr., R. K. Ulrich, and G. W. Simon, 1977, Astrophys. J. **218**, 901.
Rogov, E. V., and P. E. Spivak, 1978, JETP Lett. **28**, 303.
Rolfs, C., 1973, Nucl. Phys. A **217**, 29.
Rolfs, C., 1979, Bethe—40th Anniversary Symposium; and private communication.
Rolfs, C., 1981 (private communications).
Rolfs, C., and R. E. Azuma, 1974, Nucl. Phys. A **227**, 291.
Rolfs, C., and H. P. Trautvetter, 1978, Annu. Rev. Nucl. Particle Sci. **28**, 115.
Rolfs, C., and W. Rodney, 1974, Nucl. Phys. A **235**, 450.
Ross, J. E., and L. H. Aller, 1976, Science **191**, 1223.
Rosznyai, B., 1980 (private communications).
Rowley, J. K., 1974, in *Leningrad Seminar on Particle Acceleration and Nuclear Reactions in Space,* edited by G. E. Kocharov and V. A. Dergachev, p. 111.
Rowley, J. K., 1978, in *Proceedings of Informal Conference on Status and Future of Solar Neutrino Research,* edited by G. Friedlander (Brookhaven National Laboratory Report No. BNL 50879), Vol. 1, p. 265.
Rowley, J. K., B. T. Cleveland, R. Davis, Jr., W. Hampel, and T. Kirsten, 1980, "The Ancient Sun" in *Geochemica Et Cosmo Chemica Acta,* edited by R. O. Pepin, J. A. Eddy, and R.B. Merrill, Supp. 13, p. 45.
Rustach, B. M., 1972, Phys. Rev. D **5**, 1628.
Salpeter, E. E., 1968, Comments Nucl. Part. Phys. **2**, 97.
Schilling, A. E., N. F. Mangelson, K. K. Nielson, D. R. Dixon, M. W. Hill, G. L. Jensen, and V. C. Rogers, 1976, Nucl. Phys. A **263**, 389.
Scott, R. D., 1976, Nature **264**, 729.
Scott, R. D., 1978, in *Proceedings of Informal Conference on Status and Future of Solar Neutrino Research,* edited by G. Friedlander (Brookhaven National Laboratory Report No. BNL 50879), Vol. 1, p. 293.
Sears, R. L., 1964, Astrophys. J. **140**, 477.
Sosnovskii, A. N., P. E. Spivak, Yu. A. Prokof'ev, I. E. Kutikov, and Yu. P. Dobrynin, 1959, Sov. Phys.—JETP **8**, 739 [Nucl. Phys. **10**, 395 (1959)].
Tassoul, M., 1980, Astrophys. J. Suppl. **43**, 469.
Tombrello, T. A., 1967, in *Nuclear Research with Low Energy Accelerators,* edited by J. B. Marion and D. M. Van Patter (Academic, New York), p. 195.
Tombrello, T. A., and P. D. Parker, 1963, Phys. Rev. **131**, 2582.
Trautvetter, H. P., 1981, Comments Nucl. Part. Phys. **10**, 123.
Ulrich, R. K., 1970, Astrophys. J. **162**, 993.
Ulrich, R. K., 1971, Astrophys. J. **168**, 57.
Ulrich, R. K., 1974, Astrophys. J. **188**, 369.
Ulrich, R. K., and E. J. Rhodes, Jr., 1977, Astrophys. J. **218**, 521.
Ulrich, R.K., 1982, Astrophys. J. (in press).
Vandakurov, Yu. V., 1967, Astron. Zh. **44**, 786.
Vaughn, F. J., R. A. Chalmers, D. Kohler, and L. F. Chase, Jr., 1970, Phys. Rev. C **2**, 1657.
Vonach, H., P. Glässel, E. Huenges, P. Maier-Komor, H. Rösler, H. J. Scheerer, H. Paul, and D. Semrad, 1977, Nucl. Phys. A **278**, 189.
Warters, W. D., W. A. Fowler, and C. C. Lauritsen, 1953, Phys. Rev. **91**, 917.
Wasserburg, G. J., D. A. Papanastassiou, and T. Lee, 1980, in *Early Solar System Processes and the Present Solar System,* Corso Soc. Italiana di Fisica, Bologna.
Wasserburg, G. J., F. Tera, D. A. Papanastassiou, and J. C. Huneke, 1977, Earth Planet. Sci. Lett. **35**, 294.
Wiezorek, C., H. Krawinkel, R. Santo, and L. Wallek, 1977, Z. Phys. A **282**, 121.
Williams, R. D., and S. E. Koonin, 1981, Phys. Rev. C **23**, 2773.
Willson, R. C., S. Gulkis, M. Janssen, H. S. Hudson, and G. A. Chapman, 1981, Science **211**, 700.
Willson, R. C., C. H. Duncan, and J. Geist, 1980, Science **207**, 177.
Willson, R. C., and J. R. Hickey, 1977, in *The Solar Output and its Variation,* edited by O. R. White (Colorado Associated Universities, Boulder), p. 112.
Withbro, G. L., 1971, *Menzel Symposium on Solar Physics, Atomic Spectra, and Gaseous Nebulae* (NBS Special Report No. 353), p. 127.
Zyskind, J. L., and P. D. Parker, 1979, Nucl. Phys. A **320**, 404.